İSTANBUL TECHNICAL UNIVERSITY ★ INFORMATICS INSTITUTE

IMPLEMENTATION OF RELIABILITY BASED DESIGN OPTIMIZATION TECHNIQUES FOR AEROSPACE STRUCTURES

M.Sc. Thesis by
Çağrı ULUCENK

Department : **Informatics**

Programme : **Computational Science and Engineering**

JUNE 2009

İSTANBUL TECHNICAL UNIVERSITY ★ INFORMATICS INSTITUTE

IMPLEMENTATION OF RELIABILITY BASED DESIGN OPTIMIZATION TECHNIQUES FOR AEROSPACE STRUCTURES

M.Sc. Thesis by
Çağrı ULUCENK
(702061011)

Date of submission : **04 May 2009**
Date of defence examination: **09 June 2009**

Supervisor (Chairman) : **Assis. Prof. Dr. Melike NİKBAY (ITU)**
Members of the Examining Committee : **Prof. Dr. Metin DEMİRALP (ITU)**
Prof. Dr. Zahit MECİTOĞLU (ITU)

JUNE 2009

İSTANBUL TEKNİK ÜNİVERSİTESİ ★ BİLİŞİM ENSTİTÜSÜ

GÜVENİLİRLİK TABANLI TASARIM OPTİMİZASYONU TEKNİKLERİNİN HAVA-UZAY YAPILARI İÇİN UYGULANMASI

YÜKSEK LİSANS TEZİ

Çağrı ULUCENK
(702061011)

Tezin Enstitüye Verildiği Tarih : 04 Mayıs 2009
Tezin Savunulduğu Tarih : 09 Haziran 2009

Tez Danışmanı : Yrd. Doç. Dr. Melike NİKBAY (İTÜ)
Diğer Jüri Üyeleri : Prof. Dr. Metin DEMİRALP (İTÜ)
Prof. Dr. Zahit MECİTOĞLU (İTÜ)

HAZİRAN 2009

FOREWORD

I would first like to thank my mother, father and brother very much who are the primary people behind my every achievement. I wish to express my deep appreciation and gratitude to my family for their endless love, support and patience.

I would also like to thank my advisor, Assis. Prof. Dr. Melike Nikbay for her support and guidance during this work.

Many thanks and much appreciation to my dear friends, Coşar Gözükırmızı, Hamdi Nadir Tural, Ahmet Aysan and Arda Yanangönül. I am so fortunate and happy to have such valuable fellows.

I am pleased to thank Prof. Dr. Metin Demiralp for his inspiration. I am glad to be his student.

Finally, I thank all the people who try to make the justice exist.

May 2009 — Çağrı ULUCENK

Mathematician

TABLE OF CONTENTS

ABBREVIATIONS

RBDO	:	Reliability-based design optimization
RIA	:	Reliability index approach
PMA	:	Performance measure approach
FORM	:	First-order reliability method
MPP	:	Most probable point
AMV	:	Advanced mean value
CMV	:	Conjugate mean value
HMV	:	Hybrid mean value
HLRF	:	Hasofer, Lind, Rackwitz and Fiessler

LIST OF TABLES

LIST OF FIGURES

LIST OF SYMBOLS

$\mathbf{X}$	:	random parameter
$\mathbf{U}$	:	independent and standard normal random parameter
$\mathbf{T}$	:	Transformation between X- and U-spaces
$\mathbf{\Phi}$	:	Standard normal probability distribution function
$\mathbf{f_x}(\mathbf{x})$	:	Joint probability density function of the random parameters
$\beta_\mathbf{t}$	:	Target reliability index
$\mathbf{u}^*_{\mathbf{G}(\mathbf{U})=\mathbf{0}}$	:	Most probable point in first-order reliability analysis

IMPLEMENTATION OF RELIABILITY BASED DESIGN OPTIMIZATION TECHNIQUES FOR AEROSPACE STRUCTURES

SUMMARY

A deterministic design optimization does not account for the uncertainties that exist in modeling and simulation, manufacturing processes, design variables and parameters. Therefore the resulting deterministic optimal solution is usually associated with a high chance of failure.

Reliability based design optimization (RBDO) deals with obtaining optimal designs characterized by a low probability of failure. The first step in RBDO is to characterize the important uncertain variables and the failure modes which can be done using probability theory. The probability distributions of the random variables are obtained using statistical models. The whole process aims to design more reliable products.

In this work, some solution methodologies of RBDO are investigated. Performance measure approach which is one the FORM (first order reliability method) based methods is used for reliability analysis. The implemented algorithm is first verified for a benchmark problem in literature and a compromise is reached on the obtained results.

Finally, the written code is integrated with commercial softwares to solve a reliability based design optimization problem of an aircraft wing. The results are compared to the ones which were previously computed by a deterministic design optimization process. The compatible outputs indicate that integration of the code and softwares results in success.

GÜVENİLİRLİK TABANLI TASARIM OPTİMİZASYONU TEKNİKLERİNİN HAVA-UZAY YAPILARI İÇİN UYGULANMASI

ÖZET

Deterministik tasarım eniyilemesi modelleme, simulasyon, üretim süreci, tasarım değişkenleri ve parametrelerinde oluşan belirsizlikleri hesaba katamaz. Bu yüzden, ortaya çıkan en iyi deterministik çözüm genellikle yüksek oranda çöküş olasılığı taşır.

Güvenilirlik tabanlı tasarım eniyilemesi (GTTE) düşük çöküş olasılıklı en iyi tasarımı elde etmekle ilgilenir. GTTE'deki ilk adım önemli rastlantısal değişkenleri ve bunların çöküş durumlarını olasılık teorisi kullanarak belirlemektir. İstatistiki veriler kullanılarak rastlantısal değişkenlerin davranışları hakkında bilgi elde edilebilir. Tüm GTTE süreci ortaya daha güvenilir tasarımlar çıkarmayı hedefler.

Bu çalışmada, GTTE'nin belli bazı çözüm yöntemleri incelenmiştir. Birinci dereceden güvenilirlik yöntemlerine dayanan başarım ölçümü yaklaşımı, güvenilirlik çözümlemesi yapmakta kullanılmıştır. Uygulanan algoritma önce bilimsel yazından bir deneme problemi üzerinde çalıştırılmış, elde edilen sonuçların bilimsel yazındaki sonuçlarla uyuştuğu gözlemlenmiştir.

Son olarak, yazılan kod, basit bir uçak kanadının güvenilirlik tabanlı tasarım eniyilemesi problemini çözmek için ticari yazılımlarla birleştirilmiştir. Daha önce elde edilen deterministik eniyileme sonuçlarıyla karşılaştırılan sonuçların uyumlu ve mantıklı çıkması, kod ve yazılımların birleştirilmesinin başarıyla sonuçlandığını göstermiştir.

1. INTRODUCTION

1.1 Background and Literature Review of Reliability and Optimization

The term *reliability*, in the modern understanding by specialists in engineering, system design, and applied mathematics, is an acquisition of the 20th century. It appeared because various technical equipment and systems began to perform not only important industrial functions but also served for the security of people and their wealth.

Initially, reliability theory was developed to meet the needs of the electronics industry. This was a consequence of the fact that the first complex systems appeared in this field of engineering. Engineering design problems often involve uncertainties stemming from various sources such as manufacturing process, material properties and operating environment. Because of these uncertainties, the performance of a design may differ significantly from its nominal value. Traditional deterministic designs obtained without any consideration of uncertainties can be sensitive to the variations. For example, a system can be risky (with high chance of failure) if its design has low likelihood of constraint satisfaction. On the other hand, a system can be uneconomic and conservative if the safety factor of the design is much larger than required. Therefore it is important to consider uncertainties during the engineering design process and develop computationally efficient techniques that enable engineers to make both optimal and reliable design decisions. These factors lead to the development of a specialized applied mathematical discipline which allowed one to make a priori evaluation of various reliability indexes at the design stage, to choose an optimal system structure, to improve methods of maintenance, and to estimate the reliability on the basis of special testing or exploitation.

There are two categories of methodologies handling uncertainties in engineering design: reliability based design and robust design. An optimization process that accounts for feasibility under uncertainty is commonly referred to as reliability based design optimization (RBDO). RBDO ensures that the design is feasible regardless of the variations of the design variables and parameters. Robust design focuses on minimizing the variance of the design outcome under the variations of design variables and parameters. RBDO is the focus of this work.

In general, a RBDO model includes deterministic design variables, random design variables and random parameters. A deterministic design variable is a design variable to be designed with negligible uncertainties. A random design variable is a variable to be designed with uncertainty property being considered (usually the mean of the variable is to be determined) while a random parameter can not be controlled. The probability distributions can be used to describe the stochastic nature of the random design variables and random parameters, where the variations are represented by standard deviations which are assumed to be constant. Thus, a typical RBDO problem can be defined as a stochastic optimization model with the performance measure over the mean values of design variables (deterministic and stochastic) is to be optimized, subject to probabilistic constraints.

Reliability analysis and optimization are two essential components of RBDO: (1) Reliability analysis focuses on analyzing the probabilistic constraints to ensure that the reliability levels are satisfied; (2) Optimization seeks for the optimal performance subjected to the probabilistic constraints. Extensive research has been done to explore various efficient reliability analysis techniques including expansion methods, approximate integration methods, sampling methods and "Most Probable Failure Point" (MPP) based methods. Among those, MPP-based approaches have attracted more attention as they require relatively less computational effort while still producing results with acceptable accuracy compared to the other three approaches [7,8].

Since expansion methods such as Taylor expansion method or Neumann expansion method needs high-order partial sensitivities to calculate the probability of failure, it is not appropriate for large-scale engineering application. There are also other expansion methods such as Karhunen-Loeve (KL) and Polynomial Chaos Expansion (PCE). In the KL expansion, truncated KL series are used to represent the random field and can be implemented in the Finite Element Model, and either perturbation theory or a Neuman expansion can be applied to determine the response variability. The KL expansion requires the covariance function of the process to be expanded in which a-priori knowledge of the eigen functions is required. Polynomial Chaos Expansion (PCE) is a method that has been used to explore the variability of response in control [9, 10], computational fluid dynamics [11, 12] and buckling problems [13]. It is implemented in a similar way to the KL expansion, but does not require expansion of the covariance functions, and is simple to implement when determining the response model. The use of PCE for the stability and control of non-linear problems has been found as an efficient method even when other techniques such as Lyapunov's method have failed [9]. The potential of PCE is tremendous because of its simplicity, versatility and computational efficiency within the framework of Probability Theory.

One representative method in approximate integration methods is a Point Estimation Method (PEM). This method selects experimental points first, and then conducts numerical integration by using the system responses of experimental points and corresponding weight values. As the results of numerical integration, statistical moments of the system are obtained and the probability of failure is calculated from these values by using the Pearson system. However, since the Pearson system uses only the first four moments of the system, the accuracy of the method cannot be guaranteed.

Monte Carlo Simulation(MCS), a representative method in sampling methods is widely used because it has simple formulation and it is not affected by the shape of limit state function and the number of failure regions. This method features effectiveness on problems that are highly nonlinear with respect to the uncertainty parameters. But MCS needs an excessive number of analyses, which is not adequate for practical problems. This computational cost is the most serious drawback, in particular when the reliability level is high, that is the failure probability low. Latin Hypercube Sampling (LHS), one of the other sampling methods is known that it is more efficient than the MCS.

MPP-based methods are also widely used to calculate the probability of failure. They transform original random space into standard normal random space and define the reliability index as the minimum distance between the origin of the standard normal random space and transformed failure surface. The point on the failure surface which has minimum distance is called Most Probable failure Point(MPP) and the probability of failure is determined by Probability Density Function(PDF) of normal distribution with obtained reliability index. There are two representative methods in this category: Reliability Index Approach(RIA) and Performance Measure Approach(PMA). RIA was a widely used method to handle the probabilistic constraints before the 1990s. However, RIA is not likely to find a solution when responses of limit state function are stationary or target probability of failure is too small [14]. To overcome these problems, Performance Measure Approach(PMA), which adapts a performance function instead of the reliability index [4, 15, 16], is used. RIA and PMA are based on the concept of characterizing the probability of survival by the reliability index and then performing computations based on first order reliability methods (FORM). This method approximates the reliability index and require a search for the MPP on the failure surface ($g_j = 0$) in the standard normal space. FORM employs a linear approximation of the limit state function at the MPP and is considered accurate as long as the curvature is not too large. On the other hand, second order reliability method (SORM) features an improved accuracy by using a quadratic approximation.

Another research issue in RBDO is to investigate the integration of reliability analysis and optimization, using nested double-loop strategy or decoupled double-loop strategy. Nested double-loop methods treat the reliability analysis as the inner loop analyzing the probabilistic constraint satisfaction given the solutions provided by the outer optimizer which locates the optimal solution iteratively. As a result, nested double-loop methods are computationally expensive for a complex engineering design [7, 17, 18]. Therefore, decoupled double-loop methods have been developed to address the computational challenges [4, 7, 18–22]. However, since the reliability analysis dominates the use of computational resources during the entire design process, the efficiency of RBDO is still of great concern. What is added importance of improving RBDO is the increased attention to integrate reliability analysis with multi-disciplinary optimization.

A survey of the literature reveals that the various RBDO methods can be divided into two broad categories: Nested double-loop RBDO and decoupled double-loop RBDO models.

Nested Double-Loop RBDO Model

Traditional approaches for solving RBDO problems employ a double-loop strategy in which the reliability analysis and the optimization are nested [23]. As shown in figure 1.1 [8], the inner loop is the reliability assessment of probabilistic constraints, which involves an iterative procedure; the outer loop optimizer controls the optimization search process, which calls the inner loop repeatedly for gradient or function assessments. Since reliability analysis is needed for every probabilistic constraint, the efficiency of nested methods is especially low when there are many probabilistic constraints.

Decoupled Double-Loop RBDO Model

To improve the efficiency of a probabilistic analysis, some methods decouple the optimization loop and the reliability analysis loop. These methods include MPP based decoupling methods, first order Taylor series approximation and derivative based decoupling methods. Each of these methods is reviewed in the following sections.

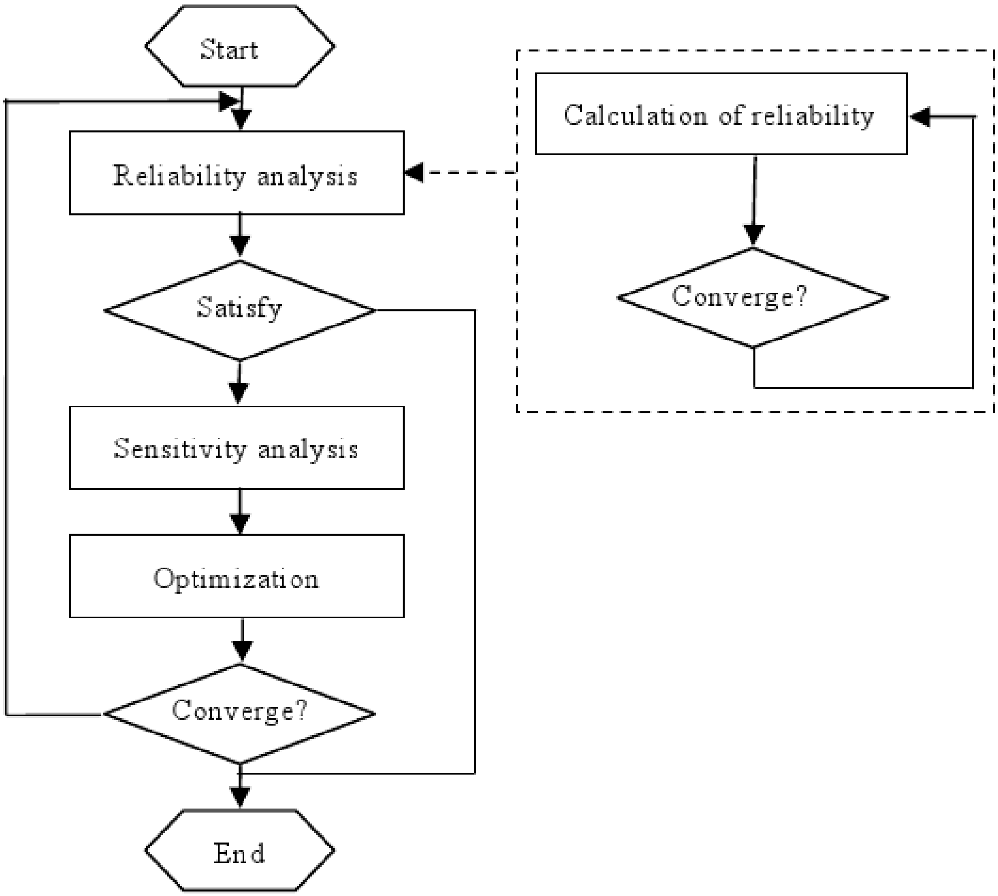

Figure 1.1: Flowchart of the nested double-loop strategy [8]

MPP Based Decoupling Approaches

The concept of MPP is widely used in RBDO to decouple the reliability analysis loop and optimization loop. The MPP (or called design point) is defined as a particular point in the design space that can be used to evaluate the probability of system failure.

Du and Chen [18] develop a decoupled double-loop method termed Sequential Optimization and Reliability Assessment (SORA). As shown in figure 1.2 [18], the SORA method employs a sequential strategy where a series of optimization and reliability assessments are employed in turn. In each circle, optimization and reliability assessment are decoupled from each other so that no reliability assessment is required within the optimization loop. The reliability assessment is only conducted after the optimization loop is finished. The key concept of SORA is to drive the boundaries of violated probabilistic constraints to the feasible region based on the reliability information obtained in the previous cycle. Hence, the design is improved from cycle to cycle and the computation efficiency is improved by decoupling the reliability analysis from the optimization loop.

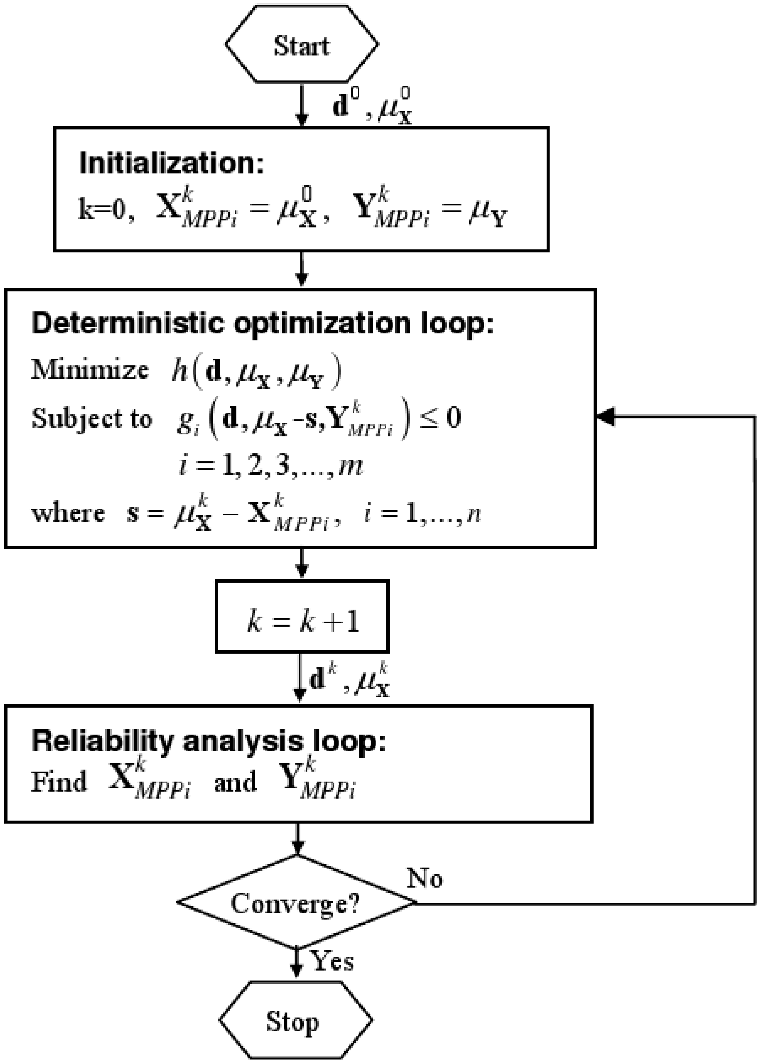

Figure 1.2: Flowchart of SORA [18]

Thanedar and Kodiyalam [19] also explore the use of MPP for RBDO and propose a double-design-variable method to decouple the reliability analysis and optimization loops, where one vector is used for the mean values of the original random design variables and another vector is introduced to contain the

MPP values. One drawback of this method is that it doubles the dimension of the design variables [8]. Thus the applicability of this method to large scale design is questionable. Another decoupling approach is developed by Sues and Cesare in which MPPs are computed using the updated design variables in each optimization iteration [25]. As stated by Liu et al. [8], one potential issue with this approach is that the MPPs obtained may not be accurate.

First order Taylor series approximation

Other than MPP based decoupling approaches, first order Taylor series approximation has been used to replace the probabilistic constraints. The reliability analysis is not performed inside the optimization loop as in nested double-loop RBDO approaches so that there are no reliability evaluations within the optimization loop. One example is design potential method (DTM) [20], where the search direction for optimization is determined using the first-order Taylor series approximation. The Taylor expansion is written at the so called design potential point (DPP), which is defined as the design point derived from the MPP using FORM. Zhou and Mahadevan [7] decouple the optimization and reliability analysis by first-order Taylor series expansion, where the approximation of the probabilistic constraints is based on the reliability analysis results.

Derivative based decoupling approaches

Chen et al. [21] propose the Single-loop Single Variable (SLSV) approach, in which the optimization and reliability analysis are decoupled. The derivatives are calculated before the optimization and then used to drive the optimal solution to the feasible region. Traditional Approximation Method (TAM) evaluates the functions and their derivatives first which are then used to solve an approximate optimization problem iteratively until convergence [17]. Choi and Youn [4] apply hybrid method which combines the SLSV and MPP in RBDO to improve the optimization efficiency.

With the decoupling strategies, the reliability analysis loop and optimization loop are included in the same cycle sequentially instead of being nested. Clearly, the decoupling methods reduce the computational effort greatly comparing to the nested double-loop methods in general.

Reliability methods are becoming increasingly popular in the aerospace, automotive, civil, defense, and power industries because they provide design of safer and more reliable products at lower cost than traditional deterministic approaches. These methods have helped many companies improve dramatically their competitive position and save billions of dollars in engineering design and warranty costs. To name a few, recent successful applications of reliability design in the mentioned industries involve advanced systems such as space shuttle, aerospace propulsion, nanocomposite structures, and bioengineering systems.

Design optimization of complex aircraft structures for maximum performance and minimum cost has been a challenging research area for aircraft manufacturer companies in recent years. In that context, a previous work by Nikbay et al. [6] includes evaluation of a single discipline optimization problem on a generic three dimensional wing geometry by employing Catia and Abaqus as two of the most commonly used structural engineering tools for computer aided engineering in aerospace industry. A practical optimization methodology was created as a commercial optimization software, Modefrontier was coupled by this finite element based framework for its gradient-based optimization algorithm options. Three similar but distinct optimization problems were investigated. The first case leant on the structural optimization of a statically loaded wing where as the second case leant on the optimization of modal frequencies and deflections of that wing. Finally, third case was a combination of both the first and the second cases previously mentioned. The optimization criteria made use of mass, fundamental frequency, maximum deflection and maximum stress of the structure. The design variables were chosen as the thicknesses of all structural members and geometric positions of selected rib and spar members. Abstract optimization variables were introduced to reduce the number of optimization variables which were still enough to relate the full set of design variables to the optimization criteria to update the geometry.

1.2 Purpose and Outline of the Thesis

Main purpose of this work is to learn and take advantage of the reliability based design optimization concept and underline its importance for the practical industrial applications. In this context, first step is taken by evaluating an aircraft wing [6] optimization problem in terms of RBDO.

In the second chapter, reliability based design optimization is introduced and its main differences with respect to deterministic optimization are explained. Mathematical approaches about reliability analysis are given and the related methods are presented.

Third chapter covers the first verification of implemented algorithm. A benchmark problem with a cantilever beam design from the literature is solved and the methodology is validated. Different reliability analysis methods are compared in terms of efficiency.

Fourth chapter includes the integration of the written code and commercial softwares for the optimization problem presented formerly by Nikbay et al. [6]. Reliability based optimization of a simple aircraft wing structure is performed and results are compared to the ones of the deterministic optimization [6].

In the fifth chapter, conclusions are drawn based on the experiences.

2. RELIABILITY BASED DESIGN OPTIMIZATION

2.1 Introduction

In this chapter, the concept of reliability based design optimization is presented. RBDO formulation and all related mathematical topics are introduced. Before proceeding to the reliability-based design optimization, formulation of the deterministic design optimization is first given below.

2.2 Deterministic Design Optimization Formulation

A typical deterministic design optimization problem can be formulated as:

$$\begin{aligned} min \quad & f(\mathbf{d},\mathbf{p},\mathbf{y}(\mathbf{d},\mathbf{p})) \\ s.t. \quad & g_i^R(\mathbf{d},\mathbf{p},\mathbf{y}(\mathbf{d},\mathbf{p})) \geq 0, \qquad i = 1,\cdots,N_{hard}, \\ & g_j^D(\mathbf{d},\mathbf{p},\mathbf{y}(\mathbf{d},\mathbf{p})) \geq 0, \qquad j = 1,\cdots,N_{soft}, \\ & \mathbf{d}^l \leq \mathbf{d} \leq \mathbf{d}^u \end{aligned} \tag{2.1}$$

where $\mathbf{d}$ are the design variables and $\mathbf{p}$ are the fixed parameters of the optimization problem. g_i^R is the i^{th} hard constraint that models the i^{th} critical failure mechanism of the system (e.g., stress, deflection, loads, etc). g_j^D is the j^{th} soft constraint that models the j^{th} deterministic constraint due to other design considerations (e.g., cost, marketing, etc). The design space is bounded by $\mathbf{d}^l$ and $\mathbf{d}^u$. If $g_i^R < 0$ at a given design $\mathbf{d}$ then the artifact is said to have failed with respect to the i^{th} failure mode. $\mathbf{y}(\mathbf{d},\mathbf{p})$ is a function which is defined to predict performance characteristics of the designed product. Obviously, equality constraints could also be included in the optimization formulation.

Although a clear distinction is made between hard and soft constraints, deterministic design optimization treats both these type of constraints similarly, and the failure of the designed product due to the presence of uncertainties is not taken into consideration.

2.3 Reliability-Based Design Optimization Formulation

The basic idea in reliability based design optimization is to employ numerical optimization algorithms to obtain optimal designs ensuring reliability. When the optimization is performed without accounting the uncertainties, certain hard constraints that are active at the deterministic solution may lead to system failure. RBDO makes the solution locate inside the feasible region.

A reliability-based design optimization problem can be formulated as follows:

$$\begin{aligned} &min && f(\mathbf{d},\mathbf{p},\mathbf{y}(\mathbf{d},\mathbf{p})) && \\ &s.t. && \mathbf{g}_i^{prob}(\mathbf{X},\boldsymbol{\eta}) \geq 0, && i = 1,\cdots,N_{prob}, \\ & && g_j^{det}(\mathbf{d},\mathbf{p},\mathbf{y}(\mathbf{d},\mathbf{p})) \geq 0, && j = 1,\cdots,N_{det}, \\ & && \mathbf{d}^l \leq \mathbf{d} \leq \mathbf{d}^u && \end{aligned} \quad \textbf{(2.2)}$$

where probabilistic constraints are represented with the superscript "*prob*" while deterministic constraints are represented with the superscript "*det*". It is clear that the hard constraints in deterministic design optimization formulation correspond to probabilistic constraints and soft contraints correspond to deterministic constraints in this formulation. Moreover, $\mathbf{X}$ denotes the vector of continuous random variables with known (or assumed) joint cumulative distribution function (CDF), $F_X(x)$. The design variables, $\mathbf{d}$, consist of either distribution parameters θ of the random variables $\mathbf{X}$, such as means, modes, standard deviations, and coefficients of variation, or deterministic parameters, also called limit state parameters, denoted by η. The design parameters $\mathbf{p}$ consist of either the means, modes, or any first order distribution quantities of certain random variables. Mathematically, this can be represented by the statement $[p,d] = [\theta,\eta]$ ($\mathbf{p}$ is a subvector of θ). Additionally, $\mathbf{g}_i^{prob}$ can be written as given below:

$$g_i^{prob} = P_{allow_i} - P_i \quad or \quad \beta_i - \beta_{req_i} \quad \textbf{(2.3)}$$

where P_i and β_i are the probability of failure and reliability index respectively due to i^{th} failure mode at the given design. On the other hand, P_{allow_i} and β_{req_i} are the allowable probability of failure and required (target) reliability index for this failure mode. The equation regarding the relationship between the probability of failure and reliability index is

$$P_f \approx \Phi(-\beta) \tag{2.4}$$

where $\mathbf{\Phi}$ is the standard normal cumulative distribution function (CDF). The probability of failure P_i is given by

$$P_i = \int_{g_i(x,\eta)\leq 0} f_X(x)dx, \tag{2.5}$$

where $f_X(x)$ denotes the joint probability density function (PDF) of $\mathbf{X}$ and $g(x,\eta) \leq 0$ represents the failure domain.

2.4 Reliability Analysis

Since equation (**2.5**) can not be evaluated analytically in most cases, two representative MPP-based reliability analysis methods can be used to calculate the probability of failure; *Reliability Index Approach (RIA)* and *Performance Measure Approach (PMA)*. Although PMA is taken as the main methodology for this work, RIA is also investigated.

Both of these methods estimate the probability of failure by the reliability index and then perform computations based on first order reliability methods (FORM). Two representations of the reliability analysis can be seen in figures 2.1 [1] and 2.2 [2]. In order to evaluate the reliability index for the limit state function, FORM requires the transformation of the random variables vector $\mathbf{X}$ into the standard normal space:

$$\mathbf{U} = T(\mathbf{X}) \tag{2.6}$$

After the transformation, the components of $\mathbf{U}$ are normally distributed with zero means and unit variance and are statistically independent. Rosenblatt transformation [33] is preferred in this work among possible approaches.

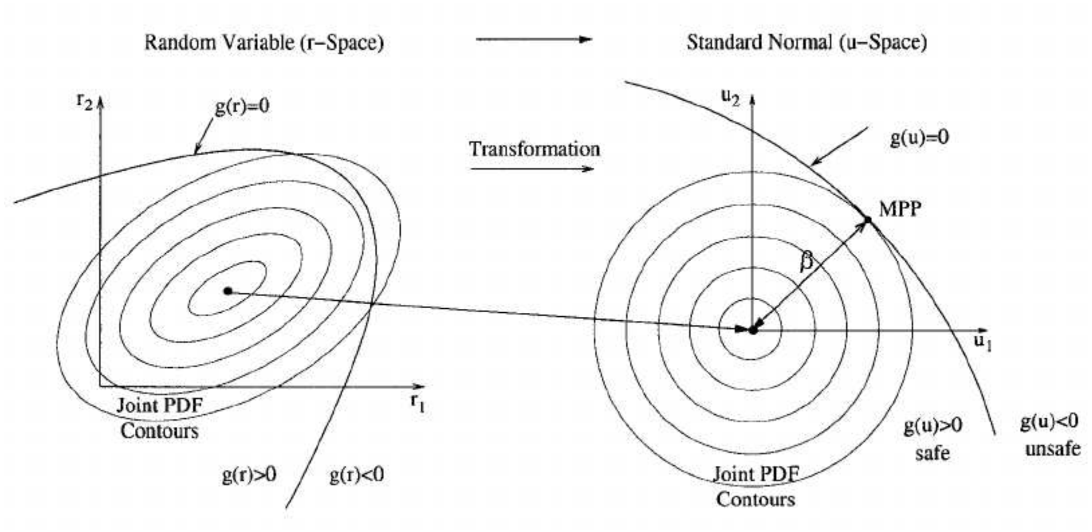

Figure 2.1: Overview of FORM process [1]

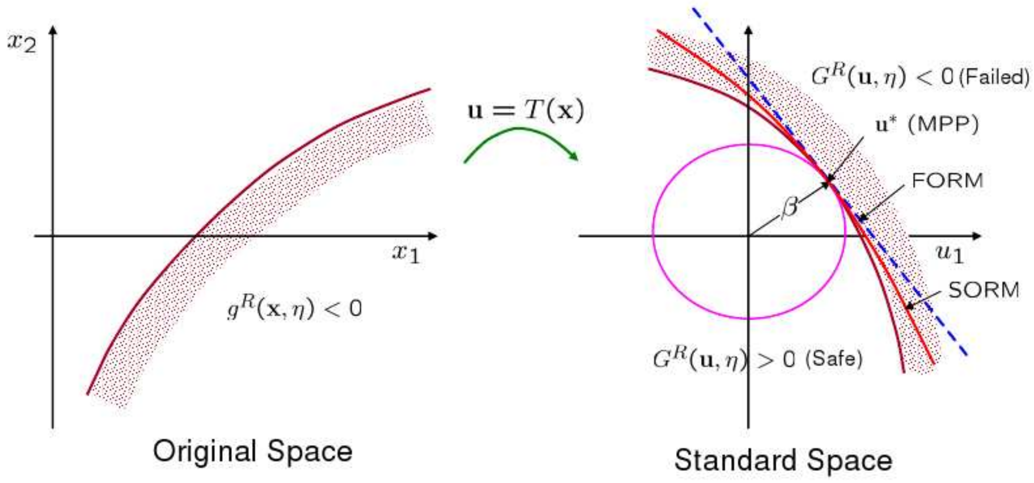

Figure 2.2: Reliability Analysis [2]

2.4.1 Rosenblatt Transformation

The Rosenblatt transformation [33] is a set of operations that permits the mapping of jointly distributed, continuous valued random variables and their realizations from the space of an arbitrary joint probability distribution into the space of uncorrelated, standard normal random variables. Let $X_1, \ldots, X_n$ be a collection of arbitrarily, jointly distributed random variables with known marginal and conditional cumulative distribution functions (CDF), $F_{X_1}(x_1), F_{X_2|X_1}(x_2|x_1)$, etc. Then the sequence of operations:

$$\begin{aligned}
U_1 &= F_{X_1}(x_1), & Z_1 = \Phi^{-1}(U_1) \\
U_2 &= F_{X_2|X_1}(x_2|x_1), & Z_2 = \Phi^{-1}(U_2) \\
&\vdots \\
U_n &= F_{X_n|X_1 \dots X_{n-1}}(x_n|x_1,\dots,x_{n-1}), & Z_n = \Phi^{-1}(U_n)
\end{aligned} \tag{2.7}$$

transform the original random variables, first into a sequence of independent uniform[0, 1] random variables, $U_1,\dots,U_n$, then into the sequence uncorrelated, standard normal random variables, $Z_1,\dots,Z_n$. The function $\Phi(.)$ is the standard normal CDF.

The transformation T can be written down explicitly in several cases. When $F(x_1,\dots,x_k)$ is a normal distribution with mean $M = (\mu_1,\dots,\mu_k)$ and covariance matrix $\Lambda = \lambda_{ij},\ i,j = 1,\dots,k$. Let $\Lambda^{(r)} = \lambda_{ij},\ i,j = 1,\dots,r \le k$, and $\Lambda_{ij}^{(r)}$ be the cofactor of λ_{ij} in $\Lambda^{(r)}$, then the transformation T is given by

$$\begin{aligned}
F_1(x_1) &= \Phi\left(\frac{x_1-\mu_1}{\sqrt{\lambda_{11}}}\right), \\
F_2(x_2|x_1) &= \Phi\left(\frac{x_2-\mu_2+(\Lambda_{21}^{(2)}/\Lambda_{22}^{(2)})(x_1-\mu_1)}{\sqrt{\Lambda^{(2)}/\Lambda_{22}^{(2)}}}\right), \\
&\vdots \\
F_k(x_k|x_{k-1},\dots,x_1) &= \Phi\left(\frac{x_k-\mu_k+\sum_{j=1}^{k-1}(\Lambda_{kj}/\Lambda_{kk})(x_j-\mu_j)}{\sqrt{\Lambda/\Lambda_{kk}}}\right)
\end{aligned} \tag{2.8}$$

Let $F(x_1,x_2)$ be a normal distribution with means μ_1,μ_2, variances σ_1^2,σ_2^2 and correlation coefficient ρ. The transformation can then be written as

$$\begin{aligned}
F_1(x_1) &= \Phi\left(\frac{x_1-\mu_1}{\sigma_1}\right), \\
F_2(x_2|x_1) &= \Phi\left(\frac{x_2-\mu_2+\frac{\rho\sigma_1}{\sigma_2}(x_1-\mu_1)}{\sigma_2\sqrt{1-\rho^2}}\right)
\end{aligned} \tag{2.9}$$

This transformation makes it possible to take advantage of the useful properties of the standard normal space which include rotational symmetry, exponentially decaying probability density in the radial and tangential directions, and the availability of formulas for the probability contents of specific sets, including the half space, parabolic sets, and polyhedral sets.

After reliability analysis is done, which means a new MPP is found, inverse transformation has to be performed in order to calculate the new design point in the original design space. This inverse transformation can be represented as follows:

$$\mathbf{x}_{new} \approx \mathbf{x}_{mean} + \mathbf{J}^{-1}(\mathbf{u}_0 - \mathbf{u}_{new}) \qquad \textbf{(2.10)}$$

where $\mathbf{x}_{new}$ and $\mathbf{u}_{new}$ denote the new design point in the original design space and the new MPP in standard normal space, respectively. On the other hand, $\mathbf{x}_{mean}$ is the mean value vector of the random variables and $\mathbf{u}_0$ is the vector which represents the origin. $\mathbf{J}^{-1}$ is the inverse of the Jacobian transformation matrix.

2.4.2 Reliability Index Approach

Reliability Index Approach (RIA) can be formulated as follows:

$$\begin{aligned} &min \quad \|\mathbf{U}\| \\ &s.t. \quad G(\mathbf{U}) = 0 \end{aligned} \qquad \textbf{(2.11)}$$

where $\mathbf{U}$ is the vector of random variables and G($\mathbf{U}$) is the limit state function. Most probable (failure) point (MPP) (the point on the limit state function which is closest to the origin), also called design point is the solution of the above nonlinear constrained optimization problem. To solve this problem, various algorithms have been reported in the literature. One of the approaches is *Hasofer-Lind and Rackwitz-Fiessler (HLRF)* algorithm that is based on a Newton-Raphson root solving approach. As shown in equation **(2.11)**, the reliability analysis in RIA is to minimize the distance $\|\mathbf{U}_{G(\mathbf{U})=0}\|$ in the standard normal space to the failure surface $G(U) = 0$. The iterative HLRF method is formulated as

$$\mathbf{u}_{HLRF}^{(k+1)} = (\mathbf{u}_{HLRF}^{(k)} \hat{\mathbf{n}}^{(k)})\hat{\mathbf{n}}^{(k)} + \frac{G(\mathbf{u}_{HLRF}^{(k)})}{\|\nabla_U G(\mathbf{u}_{HLRF}^{(k)})\|}\hat{\mathbf{n}}^{(k)} \qquad \textbf{(2.12)}$$

where the normalized steepest descent direction of G($\mathbf{U}$) at $\mathbf{u}_{HLRF}^{(k)}$ is defined as

$$\hat{\mathbf{n}}^{(k)} = \hat{\mathbf{n}}(\mathbf{u}_{HLRF}^{(k)}) = -\frac{\nabla_U G(\mathbf{u}_{HLRF}^{(k)})}{\|\nabla_U G(\mathbf{u}_{HLRF}^{(k)})\|} \quad \textbf{(2.13)}$$

and the second term in equation **(2.12)** is introduced to account for the fact that G($\mathbf{U}$) may not be zero.

The family of HLRF algorithms can exhibit poor convergence for highly nonlinear or badly scaled problems, since they are based on first order approximations of the constraint. Actually, these algorithms may fail to converge even for many well-scaled problems due to the similarities they share with Newton-Raphson approach, for example cycling of iterates may also occur in this method. The solution typically requires many system analysis evaluations. The situations where the optimizer may fail to provide a solution to the problem may include when the limit state surface is far from the origin in $\mathbf{U}$-space or when the case $G(\mathbf{U}) = 0$ never occurs at a particular design variable setting. For cases when $G(\mathbf{U}) = 0$ does not occur, the algorithm provides the best possible solution for the problem through,

$$\begin{aligned} &min && \|\mathbf{U}\| \\ &s.t. && G(\mathbf{U}) = \varepsilon \end{aligned} \quad \textbf{(2.14)}$$

where ε is a positive real number, which is small enough.

The reliability constraints formulated by the RIA are therefore not robust. To overcome these difficulties, Tu et al [23] provided an improved formulation to solve the RBDO problem, which is called the performance measure approach.

2.4.3 Performance Measure Approach

Reliability analysis in *Performance Measure Approach* is formulated as the inverse of reliability analysis in *RIA*. The first-order probabilistic performance measure G is obtained from a nonlinear optimization problem in U-space as:

$$\begin{aligned} &min && G(\mathbf{U}) \\ &s.t. && \|\mathbf{U}\| = \beta_t \end{aligned} \quad \textbf{(2.15)}$$

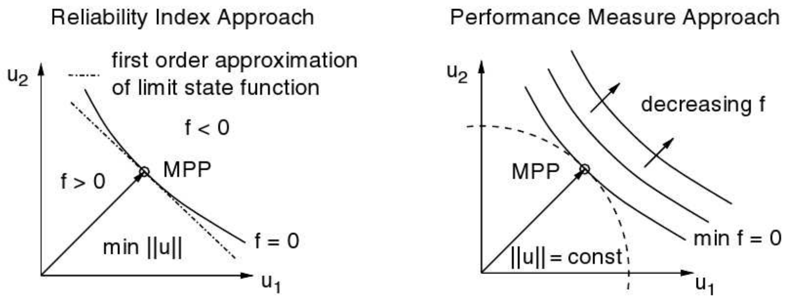

Figure 2.3: Representations of RIA and PMA [3]

where the optimum point on the target reliability surface is identified as the *MPP* $\mathbf{u}^*_{\beta=\beta_t}$ with a prescribed reliability target $\beta_t = \|\mathbf{u}^*_{\beta=\beta_t}\|$. In iterative optimization process, unlike *RIA*, only the direction vector $\mathbf{u}^*_{\beta=\beta_t}/\|\mathbf{u}^*_{\beta=\beta_t}\|$ needs to be determined by exploring the spherical equality constraint $\|\mathbf{U}\| = \beta_t$ in equation **(2.15)**. Solving RBDO by the PMA formulation is usually more efficient and robust than the RIA formulation where the reliability is evaluated directly. Also, in PMA, it can be guaranteed that the equality constraints in (**2.15**) can be satisfied in contrast to the standard formulation in (**2.11**). Rather than a general optimization algorithm, the *Advanced Mean Value (AMV)*, *Conjugate Mean Value (CMV)*, and *Hybrid Mean Value (HMV)* methods are commonly used to solve the problem in equation **(2.15)**, since they do not require a line search.

2.4.3.1 Advanced Mean Value Method

Formulation of the first-order AMV method begins with the mean value (MV) method, defined as

$$\mathbf{u}^*_{MV} = \beta_t \hat{\mathbf{n}}(\mathbf{0}) \quad \textit{where} \quad \hat{\mathbf{n}}(\mathbf{0}) = -\frac{\nabla_X G(\mu)}{\|\nabla_X G(\mu)\|} = -\frac{\nabla_U G(0)}{\|\nabla_U G(0)\|} \tag{2.16}$$

That is, to minimize the performance function G($\mathbf{U}$) (i.e., the cost function in equation **(2.15)**, the normalized steepest descent direction $\mathbf{n}(\mathbf{0})$ is defined at the mean value. The AMV method iteratively updates the direction vector of the steepest descent method at the probable point $u^{(k)}_{AMV}$ initially obtained using the

MV method. Thus, the AMV method can be formulated as

$$\mathbf{u}_{AMV}^{(1)} = \mathbf{u}_{MV}^{*}, \qquad \mathbf{u}_{AMV}^{(k+1)} = \beta_t \hat{\mathbf{n}}(\mathbf{u}_{AMV}^{(k)})$$

where

$$\hat{\mathbf{n}}(\mathbf{u}_{AMV}^{(k)}) = -\frac{\nabla_U G(\mathbf{u}_{AMV}^{(k)})}{\|\nabla_U G(\mathbf{u}_{AMV}^{(k)})\|} \tag{2.17}$$

As will be shown, this method exhibits instability and inefficiency in solving a concave function since this method updates the direction using only the current MPP.

2.4.3.2 Conjugate Mean Value Method

When applied for a concave function, the AMV method tends to be slow in the rate of convergence and/or divergent due to a lack of updated information during the iterative reliability analysis. These kinds of difficulties can be overcome by using both the current and previous MPP information as applied in the conjugate mean value (CMV) method. The new search direction is obtained by combining $\hat{\mathbf{n}}(\mathbf{u}_{CMV}^{(k-2)})$, $\hat{\mathbf{n}}(\mathbf{u}_{CMV}^{(k-1)})$ and $\hat{\mathbf{n}}(\mathbf{u}_{CMV}^{k})$ with an equal weight, such that it is directed towards the diagonal of the three consecutive steepest descent directions. That is,

$$\mathbf{u}_{CMV}^{(0)} = 0, \quad \mathbf{u}_{CMV}^{(1)} = \mathbf{u}_{AMV}^{(1)}, \quad \mathbf{u}_{CMV}^{(2)} = \mathbf{u}_{AMV}^{(2)},$$

$$\mathbf{u}_{CMV}^{(k+1)} = \beta_t \frac{\hat{\mathbf{n}}(\mathbf{u}_{CMV}^{(k)}) + \hat{\mathbf{n}}(\mathbf{u}_{CMV}^{(k-1)}) + \hat{\mathbf{n}}(\mathbf{u}_{CMV}^{(k-2)})}{\|\hat{\mathbf{n}}(\mathbf{u}_{CMV}^{(k)}) + \hat{\mathbf{n}}(\mathbf{u}_{CMV}^{(k-1)}) + \hat{\mathbf{n}}(\mathbf{u}_{CMV}^{(k-2)})\|}, \quad for \quad k \geq 2$$

where

$$\hat{\mathbf{n}}(\mathbf{u}_{CMV}^{(k)}) = -\frac{\nabla_U G(\mathbf{u}_{CMV}^{(k)})}{\|\nabla_U G(\mathbf{u}_{CMV}^{(k)})\|} \tag{2.18}$$

Consequently, the conjugate steepest descent direction significantly improves the rate of convergence, as well as the stability, compared to the AMV method for the concave performance function. However, as will be seen, CMV method is inefficient for the convex function.

2.4.3.3 Hybrid Mean Value Method

To select an appropriate MPP search method, the type of performance function must first be identified. In this work, the function type criteria are proposed by employing the steepest descent directions at the three consecutive iterations as follows:

$$\zeta^{(k+1)} = (\hat{\mathbf{n}}^{(k+1)} - \hat{\mathbf{n}}^{(k)}) \cdot (\hat{\mathbf{n}}^{(k)} - \hat{\mathbf{n}}^{(k-1)})$$

$$\begin{aligned} sign(\zeta^{(k+1)}) \quad &> \quad 0 \quad \textit{Convex type at } \mathbf{u}_{HMV}^{(k+1)} \textit{ w.r.t design } \mathbf{d} \\ &\leq \quad 0 \quad \textit{Concave type at } \mathbf{u}_{HMV}^{(k+1)} \textit{ w.r.t design } \mathbf{d} \end{aligned} \tag{2.19}$$

where $\zeta^{(k+1)}$ is the criterion for the performance function type at the $(k+1)$th step and $\hat{\mathbf{n}}^k$ is the steepest descent direction for a performance function at the MPP $\mathbf{u}_{HMV}^{(k)}$ at the kth iteration. Once the performance function type is defined, either *AMV* or *CMV* is adaptively selected for the MPP search. This numerical procedure is therefore denoted as the *hybrid mean value (HMV)* method.

The convergence criteria concerning MPP search in this method (consequently in AMV and CMV) is checked like the following: If $max(|\Delta G_{rel}^{(k+1)}|, |\Delta G_{abs}^{(k+1)}|) \leq \varepsilon$ where

$$|\Delta G_{rel}^{(k+1)}| = \left| \frac{G(\mathbf{u}_{HMV}^{(k+1)}) - G(\mathbf{u}_{HMV}^{(k)})}{G(\mathbf{u}_{HMV}^{(k+1)})} \right| \tag{2.20}$$

and

$$|\Delta G_{abs}^{(k+1)}| = |G(\mathbf{u}_{HMV}^{(k+1)}) - G(\mathbf{u}_{HMV}^{(k)})| \tag{2.21}$$

then new MPP is found. Otherwise gradient of the performance function is computed at the new $\mathbf{u}$, performance function type is determined and rest of the calculations are performed adaptively, either using AMV or CMV.

Aforementioned iterative processes in AMV and CMV methods can be observed in the written MATLAB code in a *while* loop. In each iteration, a new MPP is found. Using this newly calculated MPP, one of the above stated convergence criteria is checked. If this criterion is satisfied, *while* loop is broken and algorithm continues with the further steps. Otherwise, newly calculated MPP is assigned to the point which is used for the calculation of the new gradient vector.

The main difference between AMV and CMV methods can also be seen in that *while* loop. While AMV method uses only the current steepest descent direction, CMV method uses three consecutive directions. All remaining parts of each *while* loop was written in a similar manner.

In this work, PMA is preferred for reliability analysis calculations due to its advantages expressed above. In order to verify the implemented MATLAB code for AMV and CMV algorithms, some example problems from the literature [4] are solved and the exact results given in [4] are reached. Next section covers those problems and comparison of the results obtained.

2.4.4 Example Problems

Problem 1: Convex Performance Function

A convex function is given as [4]

$$G(\mathbf{X}) = -exp(X_1 - 7) - X_2 + 10 \tag{2.22}$$

where $\mathbf{X}$ represents the independent random variables with $X_i \sim N(6.0, 0.8)$, $i = 1,2$ and the reliability index is set to $\beta_t = 3.0$. As shown in figure 2.4 [4], the constraint in equation **(2.15)** is always satisfied and the performance function around the MPP is convex with respect to the origin of U-space. The AMV method demonstrates good convergence behavior for the convex function since the steepest descent direction $\hat{\mathbf{n}}(\mathbf{u}_{AMV}^{(k)})$ of the response gradually approaches to the MPP, as shown in figure 2.4(a). In table 2.1, the convergence rate of the AMV method is faster than that of the CMV method for the convex function because the conjugate steepest descent direction tends to reduce the rate of convergence for the convex function. Thus, for the convex performance function, the AMV method performs better than the CMV method.

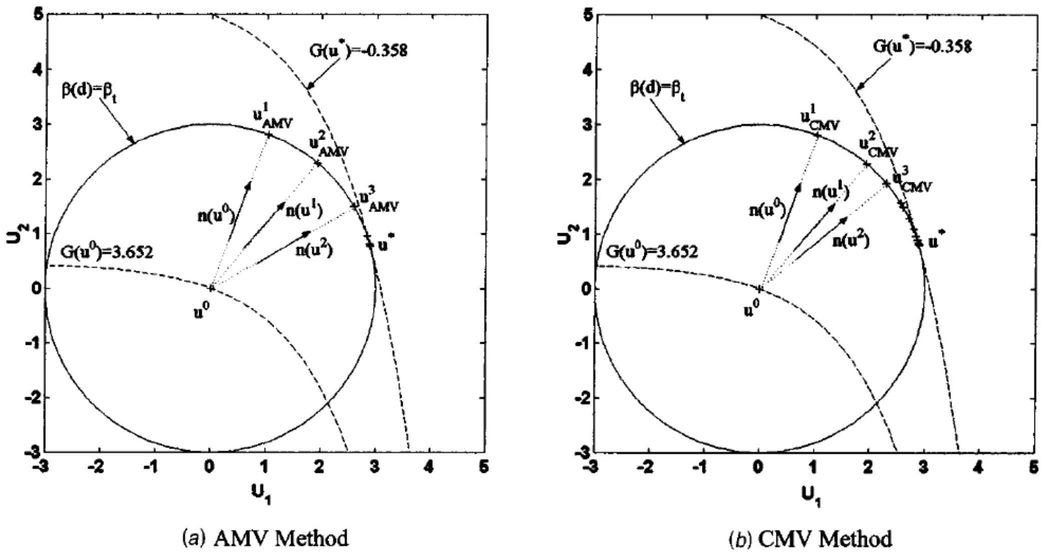

Figure 2.4: MPP search for convex performance function [4]

Table 2.1: MPP history for convex performance function

	AMV			CMV		
Iteration	X_1	X_2	G	X_1	X_2	G
1	6.829	8.252	0.905	6.829	8.252	0.905
2	7.546	7.835	0.438	7.546	7.835	0.438
3	8.077	7.203	-0.991	7.839	7.542	0.144
4	8.272	6.774	-0.341	8.043	7.260	-0.097
5	8.311	6.648	-0.357	8.165	7.035	-0.242
6	8.317	6.625	-0.358	8.234	6.877	-0.312
...					...	
11				8.310	6.651	-0.357
12				8.317	6.625	-0.358
		Converged			Converged	

Problem 2: Concave Performance Function 1

Consider the concave performance function [4]

$$G(\mathbf{X}) = [exp(0.8X_1 - 1.2) + exp(0.7X_2 - 0.6) - 5]/10 \qquad \textbf{(2.23)}$$

where $\mathbf{X}$ represents an independent random vector with $X_1 \sim N(4.0, 0.8)$ and $X_2 \sim N(5.0, 0.8)$ and the target reliability index is set to $\beta_t = 3.0$. As shown in

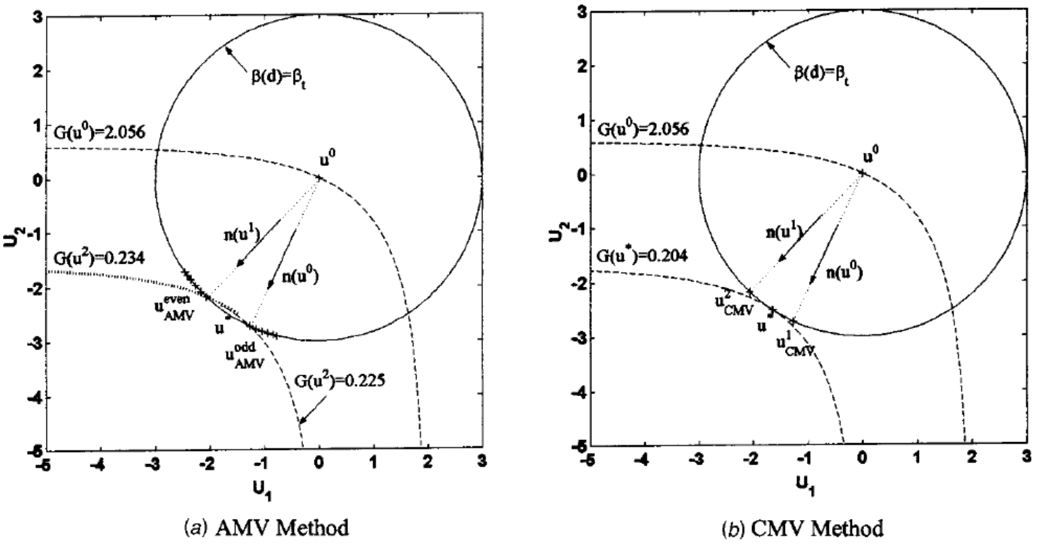

Figure 2.5: MPP search for concave performance function 1 [4]

figure 2.5 [4], the performance function around the MPP is concave with respect to the origin of U-space. The AMV method applied to the concave response diverges as a result of the oscillation observed in figure 2.5(a). As shown in table 2.2, after 34th iteration, oscillation occurs in first-order reliability analysis due to the cyclic behavior of the steepest descent directions, i.e., $\hat{\mathbf{n}}(\mathbf{u}_{AMV}^{(k)})=\hat{\mathbf{n}}(\mathbf{u}_{AMV}^{(k-2)})$ and $\hat{\mathbf{n}}(\mathbf{u}_{AMV}^{(k+1)})=\hat{\mathbf{n}}(\mathbf{u}_{AMV}^{(k-1)})$. This example shows that, unlike the convex function, the AMV method does not converge for the concave function. As presented in table 2.2, the CMV method applied to the PMA is stable when handling the concave function by using the conjugate steepest descent direction.

Problem 3: Concave Performance Function 2

A different situation is presented using another concave function with an inflected part as [4]:

$$G(\mathbf{X}) = 0.3X_1^2X_2 - X_2 + 0.8X_1 + 1 \quad \textbf{(2.24)}$$

where $\mathbf{X}$ represents the independent random variables with $X_1 \sim N(1.3, 0.55)$ and $X_2 \sim N(1.0, 0.55)$ and the target reliability of $\beta_t = 3.0$ is used. Although the AMV method has converged in this case, it requires substantially more iterations than the CMV method as can be seen in table 2.3.

Table 2.2: MPP history for concave performance function 1

	AMV			CMV		
Iteration	X_1	X_2	G	X_1	X_2	G
1	2.989	2.823	0.225	2.989	2.823	0.225
2	2.348	3.259	0.234	2.348	3.259	0.234
3	3.073	2.786	0.238	2.687	2.990	0.204
4	2.268	3.338	0.253	2.680	2.996	0.204
5	3.162	2.751	0.255			
6	2.190	3.424	0.277			
...		...				
34	1.981	3.703	0.380			
35	3.464	2.661	0.335			
...		...				
999	1.981	3.703	0.380			
1000	3.464	2.661	0.335			
		Diverged			Converged	

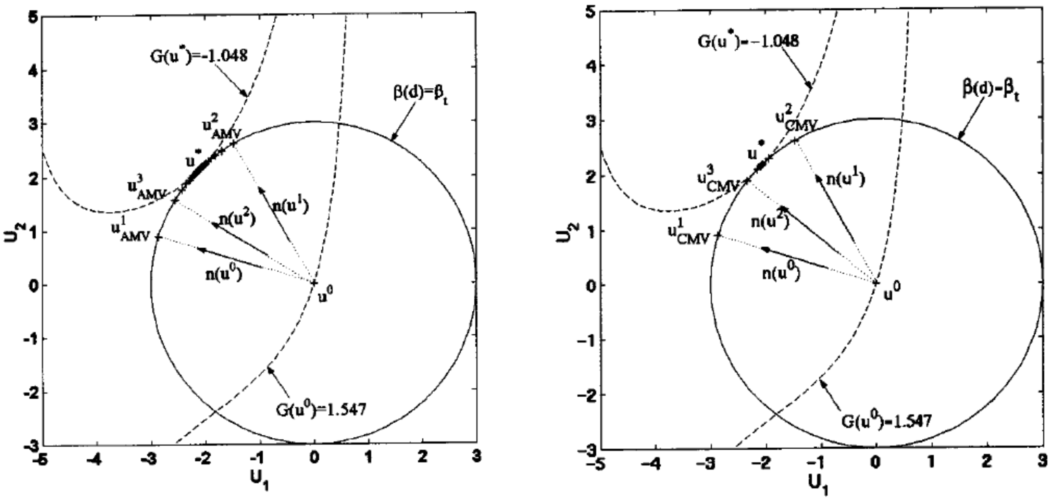

(a) AMV Method (b) CMV Method

Figure 2.6: MPP search for concave performance function 2 [4]

Similar to Problem 2, the slow rate of convergence is the result of oscillating behavior of reliability iterations (figure 2.6) [4] when using the AMV method. Based on the previous examples, it can be concluded that the AMV method

Table 2.3: MPP history for concave performance function 2

	AMV			CMV		
Iteration	X_1	X_2	G	X_1	X_2	G
1	-0.275	1.491	-0.678	-0.275	1.491	-0.678
2	0.487	2.436	-0.873	0.487	2.436	-0.873
3	-0.105	1.864	-0.997	0.016	2.036	-1.023
4	0.368	2.362	-0.959	0.232	2.257	-1.036
5	-0.035	1.969	-1.000	0.119	2.152	-1.048
6	0.303	2.315	-1.009	0.174	2.206	-1.047
7	0.009	2.028	-1.020	0.146	2.180	-1.048
8	0.260	2.281	-1.027	0.160	2.193	-1.048
9	0.041	2.067	-1.033	0.153	2.186	-1.048
10	0.230	2.256	-1.036	0.157	2.190	-1.048
11	0.064	2.094	-1.039	0.155	2.188	-1.048
...		...				
23	0.124	2.158	-1.048			
24	0.155	2.188	-1.048			
		Converged			Converged	

either diverges or performs poorly compared to the CMV method, for the concave performance function. Thus, a desirable approach is to select either the AMV or CMV methods once the type of performance function has been determined to achieve the most efficient and robust evaluation of probabilistic constraint, as explained above in the HMV method.

3. CANTILEVER BEAM PROBLEM

3.1 Introduction

This chapter includes verification of the implemented reliability analysis based MATLAB code for a benchmark problem and discussions about the results obtained.

3.2 The Algorithm

In order to solve the benchmark problem using the reliability methods mentioned in the previous chapter, a code in MATLAB was written. The figure below represents the flowchart of the algorithm:

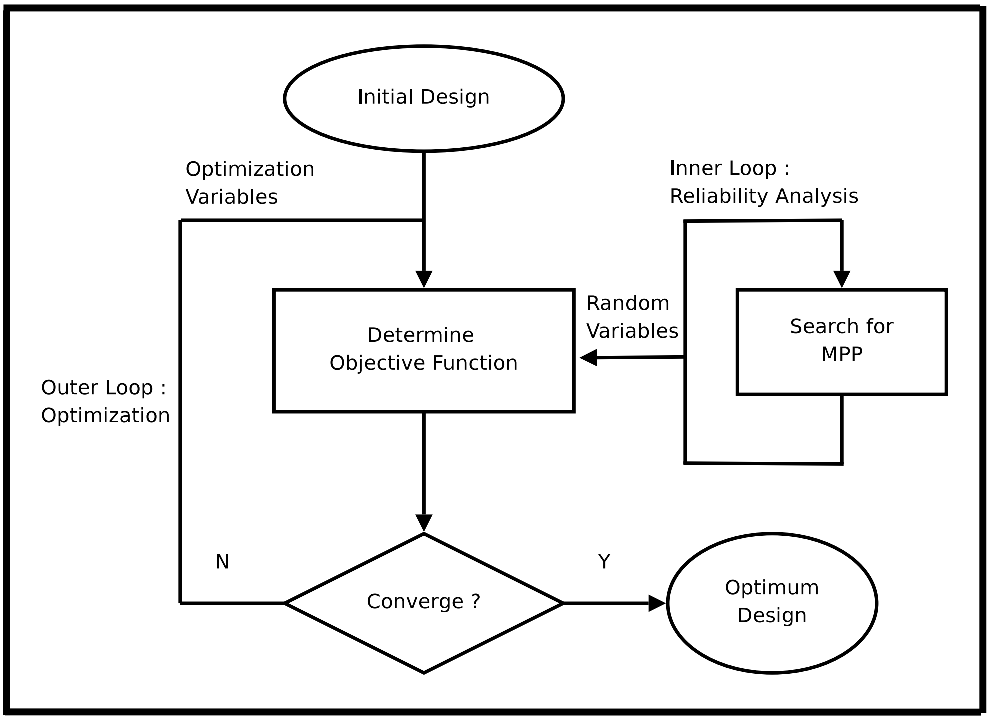

Figure 3.1: Flowchart of implemented algorithm

The deterministic optimization part of the algorithm which is shown as the outer loop in the figure is handled by a built-in MATLAB function called *fmincon*. Further information about this function is given in the next sections.

3.3 Definition of the Problem

This test problem is adapted from the reliability-based design optimization literature [5] and involves a simple uniform cantilever beam as shown in figure 3.2 [5].

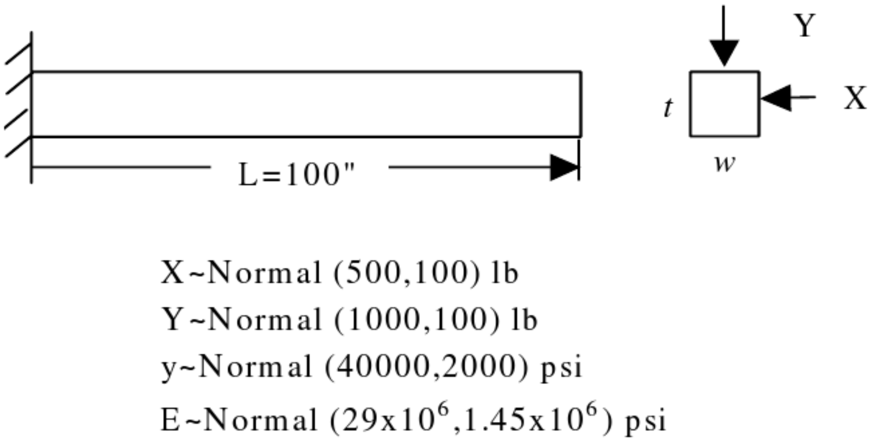

Figure 3.2: A beam under vertical and lateral bending [5]

The design problem is to minimize the weight (or, equivalently, the cross-sectional area) of a simple uniform cantilever beam subjected to a displacement constraint and a stress constraint. Random variables in the problem include the yield stress R of the beam material, the Young's modulus E of the material, and the horizontal and vertical loads, X and Y, which are modeled with normal distributions using $N(40000, 2000)$, $N(29E6, 1.45E6)$, $N(500, 100)$, and $N(1000, 100)$ respectively. Problem constants include $L = 100$in. and $D_0 = 2.2535$in. The constraints have the following analytic form:

$$stress = \frac{600Y}{wt^2} + \frac{600X}{w^2 t} \leq R \quad \textbf{(3.1)}$$

$$displacement = \frac{4L^3}{Ewt}\sqrt{\left(\frac{Y}{t^2}\right)^2 + \left(\frac{X}{w^2}\right)^2} \leq D_0 \quad \textbf{(3.2)}$$

or when scaled

$$g_S = \frac{stress}{R} - 1 \leq 0 \quad \textbf{(3.3)}$$

$$g_D = \frac{displacement}{D_0} - 1 \leq 0 \quad \textbf{(3.4)}$$

It is notable that the stress function **(3.1)** is linear in the three normal random variables and therefore the FORM solution will produce the exact result for each design. However, it is nonlinear in w and t. On the other hand, displacement function **(3.2)** is nonlinear in all the three normal random variables and therefore the FORM solution is approximate. Additionally, in this work, stress constraint is treated as *dominant constraint* for computational simplicity.

3.3.1 Deterministic Optimization Results

If the random variables E, R, X and Y are fixed at their means, the resulting deterministic design problem can be formulated as:

$$\begin{aligned} min \quad & f = wt \\ s.t. \quad & g_S \leq 0 \\ & g_D \leq 0 \\ & 1.0 \leq w \leq 4.0 \\ & 1.0 \leq t \leq 4.0 \end{aligned} \quad \textbf{(3.5)}$$

The deterministic solution is $(w,t) = (2.35, 3.33)$ with an objective function of 7.82.

3.3.2 Probabilistic Optimization Results

If the normal distributions for the random variables E, R, X, and Y are included, a probabilistic design problem can be formulated as:

$$
\begin{aligned}
min \quad & f = wt \\
s.t. \quad & \beta_D \geq 3 \\
& \beta_S \geq 3 \\
& 1.0 \leq w \leq 4.0 \\
& 1.0 \leq t \leq 4.0
\end{aligned} \qquad \textbf{(3.6)}
$$

where target reliability (β_t)=3 (probability of failure = 0.00135 if responses are normally-distributed) is being sought on the scaled constraints. Probabilistic optimizations solution is $(w,t) = (2.45, 3.88)$ with an objective function of 9.52 [5]. Both deterministic and probabilistic optimization results are obtained with perfect accuracy with the written MATLAB code. The results demonstrate that a more conservative design is needed to satisfy the probabilistic constraints.

3.4 fmincon Function in MATLAB

This function attempts to find a constrained minimum of a scalar function of several variables starting at an initial estimate. This is generally referred to as *constrained nonlinear optimization* or nonlinear programming.

fmincon uses one of three algorithms: active-set, interior point or trust region reflective. The algorithm can be chosen at the command line. These algorithms are briefly explained below:

Trust Region Reflective

To understand the trust region approach to optimization, the unconstrained minimization problem, minimize f(x), where the function takes vector arguments and returns scalars, has to be considered. Let us suppose we are at a point x in n-space and we want to improve, i.e., move to a point with a lower function value. The basic idea is to approximate f with a simpler function q, which reasonably reflects the behavior of function f in a neighborhood N around the point x. This neighborhood is the trust region.

The trust region reflective algorithm is a subspace trust region method and is based on the interior-reflective Newton method described in [34]. Each iteration involves the approximate solution of a large linear system using the method of preconditioned conjugate gradients (PCG).

Interior Point

The interior point approach to constrained minimization is to solve a sequence of approximate minimization problems. To solve the approximate problem, the algorithm uses either a Newton step or a conjugate gradient step at each iteration. Detailed information is available in [35].

Active Set

fmincon uses a *sequential quadratic programming* (SQP) method. This method attempts to solve a nonlinear program directly rather than convert it to a sequence of unconstrained minimization problems. The basic idea is analogous to Newton's method for unconstrained minimization: At each step, a local model of the optimization problem is constructed and solved, yielding a step toward the solution of the original problem. In unconstrained minimization, only the objective function must be approximated, and the local model is quadratic. In the NLP

$$\begin{aligned} &min \quad && f(x) \\ &s.t \quad && g(x) \end{aligned} \tag{3.7}$$

both the objective function and the constraint must be modeled. An SQP method uses a quadratic model for the objective function and a linear model of the constraint. A nonlinear program in which the objective function is quadratic and the constraints are linear is called a *quadratic program* (QP). A SQP method solves a QP at each iteration.

Let $x^{(k)}$ be the current estimate of a solution $x^{(*)}$, then g can be approximated by

$$g(x^{(k)} + p) = \nabla g(x^{(k)})^T p + g(x^{(k)}), \tag{3.8}$$

and so the constraint

$$g(x) = 0 \tag{3.9}$$

is replaced by

$$\nabla g(x^{(k)})^T p + g(x^{(k)}) = 0 \tag{3.10}$$

At first glance, one would expect that the quadratic objective function for the model problem would be the Taylor approximation to f:

$$f(x^{(k)} + p) = f(x^{(k)}) + \nabla f(x^{(k)})p + \frac{1}{2}p\nabla^2(x^{(k)})p. \tag{3.11}$$

However, this would be the wrong choice, because the curvature of the constraints must be captured by the model problem.

If λ^* is the Langrange multiplier corresponding to a local minimizer $x^{(*)}$ of

$$\begin{aligned} min \quad & f(x) \\ s.t \quad & g(x) = 0 \end{aligned} \tag{3.12}$$

then the Langrangian $\ell(x;\lambda^*) = f(x)$ for all feasible x. It follows that

$$\begin{aligned} min \quad & \ell(x;\lambda^*) \\ s.t \quad & g(x) = 0 \end{aligned} \tag{3.13}$$

also has x^* as a local minimizer. Here, λ^* is typically not known, but an algorithm can approximate λ^* as it approximates x^*. Given $x^{(k)}$ and $\lambda^{(k)}$, (for p near 0)

$$\ell(x^{(k)} + p; \lambda^k)) = \frac{1}{2}p\nabla^{(2)}\ell(x^{(k)};\lambda^k)p + \nabla\ell(x^{(k)};\lambda^k)p + \ell(x^{(k)};\lambda^k) \tag{3.14}$$

Then solving

$$\begin{aligned} min \quad & \frac{1}{2}p\nabla^{(2)}\ell(x^{(k)};\lambda^k)p + \nabla\ell(x^{(k)};\lambda^k)p + \ell(x^{(k)};\lambda^k) \\ s.t \quad & \nabla g(x^{(k)})^T p + g(x^{(k)}) = 0 \end{aligned} \tag{3.15}$$

yields improved values of $x^{(k)}$ and $\lambda^{(k)}$, at least when $x^{(k)}$ and $\lambda^{(k)}$ are close to x^* and λ^*, respectively.

The active set algorithm is not a large-scale algorithm. An optimization algorithm is large scale when it uses linear algebra that does not need to store, nor operate on full matrices. This may be done internally by storing sparse matrices, and by using sparse linear algebra for computations whenever possible.

In contrast, medium-scale methods internally create full matrices and use dense linear algebra. If a problem is sufficiently large, full matrices take up a significant amount of memory, and the dense linear algebra may require a long time to execute. A medium-scale algorithm has to be chosen to access extra functionality, such as additional constraint types or possibly for better performance.

3.5 Results and Discussion

First, both stress and displacement functions in the beam problem are evaluated as explained in the previous chapter and function types of both are determined as *concave* for every step in the iteration. The tables 3.1, 3.2 and 3.3 show the outputs of the algorithm for AMV, CMV methods and deterministic optimization respectively. In the tables, *beta* and P_f represent target reliability index and

Table 3.1: AMV Method for Beam Problem

$\varepsilon = 0.001$							
Beta	P_f	n_{iter}	nf_d	nf_u	w	t	f_{min}
2.0	0.0228	16	51	102	2.3021	3.8650	8.8975
2.5	0.0062	16	55	110	2.3757	3.8756	9.2073
3.0	0.0013	14	45	90	2.4460	3.8922	9.5202
3.5	2.3263e-04	15	48	96	2.5135	3.9139	9.8374
4.0	3.1671e-05	18	57	114	2.5786	3.9400	10.1598
4.5	3.3977e-06	17	54	108	2.6419	3.9700	10.4886
5.0	2.8665e-07	12	39	78	2.7062	4.0000	10.8249

corresponding probability of failure, n_{iter}, nf_d and nf_u are number of iterations, number of function evaluations in design space and number of function evaluations in standard normal space, respectively. The optimization algorithm used is

Table 3.2: CMV Method for Beam Problem

$\varepsilon = 0.001$							
Beta	P_f	n_{iter}	nf_d	nf_u	w	t	f_{min}
2.0	0.0228	17	54	54	2.3021	3.8650	8.8975
2.5	0.0062	17	59	59	2.3757	3.8756	9.2073
3.0	0.0013	16	51	51	2.4460	3.8922	9.5202
3.5	2.3263e-04	14	45	45	2.5135	3.9139	9.8374
4.0	3.1671e-05	16	55	55	2.5786	3.9400	10.1598
4.5	3.3977e-06	16	52	52	2.6419	3.9700	10.4886
5.0	2.8665e-07	14	45	45	2.7062	4.0000	10.8249

Table 3.3: Deterministic Optimization Results for the Beam Problem

n_{iter}	nf_d	w	t	f_{min}
13	42	2.3520	3.3263	7.8235

medium-scale: SQP, Quasi-Newton, line-search. In addition, w and t are the optimum values of the design variables and f_{min} is the minimum value of the objective function.

Since both constraints are concave, CMV method is expected to perform better for this problem. The obtained results also verify this expectation in terms of the function evaluation numbers in standard normal space. For every different value of target reliability index, nf_u in CMV is less than that of in AMV. Efficiency of these methods for this problem is depicted in figure 3.3. However, optimum values of design variables and minimum value of the function are equal in both methods for every *beta* value. Another important point which is illustrated in figure 3.4 is that increase in target reliability values results in increase in minimum value of the function for both AMV and CMV. This is sensible because increase in *beta* means the decrease in probability of failure and final design is less likely to fail if it is more conservative.

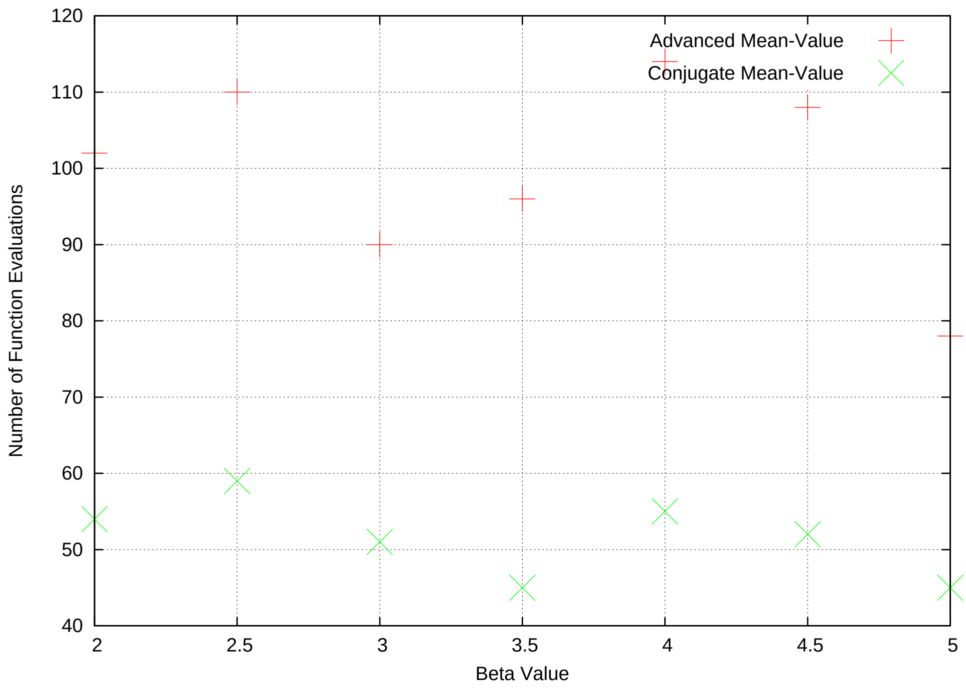

Figure 3.3: Efficiency Comparison of AMV and CMV for Various Beta Values

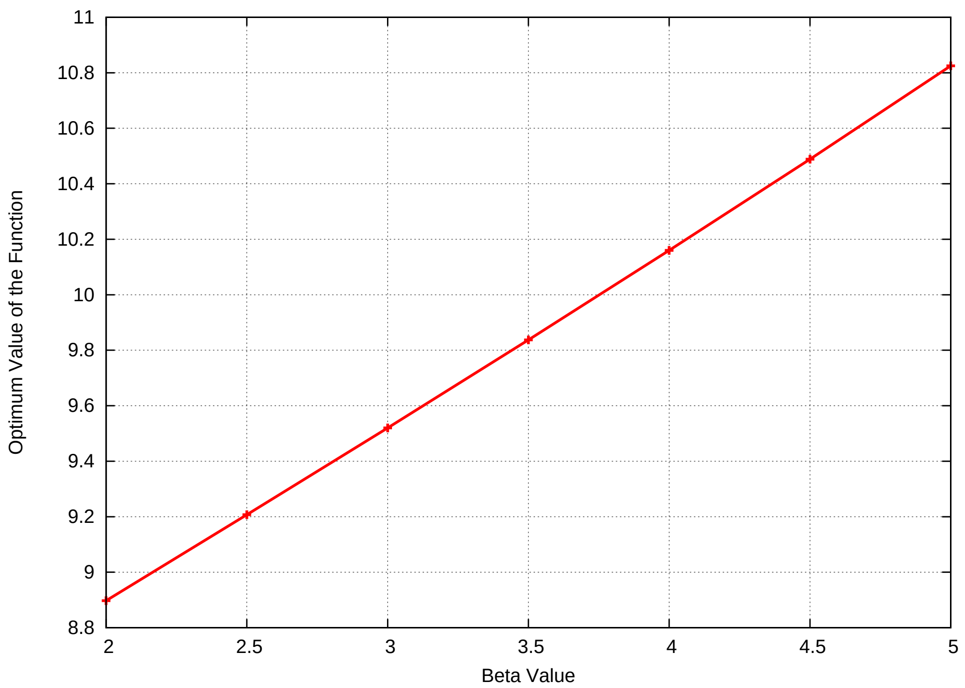

Figure 3.4: Optimum Function Values according to Different Reliability Indices

It is also observed that the iteration and function evaluation numbers in design space for probabilistic optimization are greater than those in deterministic optimization.

3.6 Verification of Algorithm's Integration with Commercial Softwares

In order to confirm that the integration of MATLAB code is done smoothly and the commercial softwares (Abaqus and ModeFrontier) are interacting well, a similar workflow for the wing problem defined in the next chapter was prepared for this beam problem. While final values of design variables were $(w,t) = (2.44, 3.89)$ and minimum value of objective function (wt) was 9.52 using only MATLAB, the prepared workflow in ModeFrontier gives $(w,t) = (2.42, 3.83)$ and $wt = 9.27$ as probabilistic optimization outputs. In short, results seem to be in good agreement. Detailed explanations about the defined workflow are given in the next chapter.

4. AIRCRAFT WING PROBLEM

4.1 Introduction

This chapter contains the reevaluation of a single discipline deterministic optimization problem on a generic three dimensional wing geometry in a previous work by Nikbay et al. [6]. In this work, the multiobjective optimization problem of [6] is solved with variables of Young's Modulus E and yield strength σ_{yield} of the material are assumed to be random. Consequently, the constraints concerning stress, displacement and frequency become probabilistic constraints. The reliability analysis part of MATLAB code and commercial software Abaqus are integrated in the framework of commercial software ModeFrontier and obtained RBDO results are compared to the deterministic ones in [6].

4.2 Definition of Multiobjective Optimization

There are many practical applications where the designer may want to optimize two or more objective functions simultaneously. These are called *multiobjective*, *multicriteria*, or *vector optimization* problems. Since the wing problem in this work is also a multiobjective optimization problem, basic terminology and solution methods for such problems are given briefly.

A multiobjective optimization problem can be defined as follows:

$$\begin{aligned} min \quad & \mathbf{f}(\mathbf{x}) = (f_1(\mathbf{x}), f_2(\mathbf{x}), \ldots, f_k(\mathbf{x})) \\ s.t. \quad & h_i(\mathbf{x}) = 0; \quad i = 1, \ldots, p \\ & g_j(\mathbf{x}) \leq 0; \quad j = 1, \ldots, m \end{aligned} \tag{4.1}$$

where k is the number of objective functions, p is the number of equality constraints, and m is the number of inequality constraints. $\mathbf{f}(\mathbf{x})$ is a k-dimensional vector of objective functions. The feasible set S (also called the feasible design space) is defined as a collection of all the feasible design points, as

$$S = \{\mathbf{x} | h_i(\mathbf{x}) \leq 0; \quad i = 1, \ldots, p; \quad and \quad g_j(\mathbf{x}) \leq 0; \quad j = 1, \ldots, m\} \tag{4.2}$$

Pareto optimality is the main solution method for the wing problem. Basically, a point x^* in the feasible design space S is called *Pareto optimal* if there is no other point $\mathbf{x}$ in the set S that reduces at least one objective function without increasing another one. This can be defined more precisely as follows:

A point x^* in the feasible design space S is Pareto optimal if and only if there does not exist another point $\mathbf{x}$ in the set S such that $\mathbf{f}(\mathbf{x}) \leq \mathbf{f}(\mathbf{x}^*)$ with at least one $f_i(\mathbf{x}) < f_i(\mathbf{x}^*)$.

Inequalities between vectors apply to every component of each vector; e.g., $\mathbf{f}(\mathbf{x}) \leq \mathbf{f}(\mathbf{x}^*)$ implies $f_1 \leq f_1^*, f_2 \leq f_2^*$, and so on. The set of all Pareto optimal points is called the *Pareto optimal set*. The above definition means that for $\mathbf{x}^*$ to be called the Pareto optimal point, no other point exists in the feasible design space S that improves at least one objective function while keeping others unchanged.

Other solution concepts related to these problems include weak pareto optimality, efficiency and dominance, utopia point, and compromise solution, nominally. Detailed explanations can be found in [36].

4.3 Aircraft Wing Design Model

A simple aircraft wing which has a NACA0012 airfoil profile is modeled parametrically in Catia V5-R16. The wing's three dimensional geometric model consists of 90 skin panels, 10 ribs and 4 spars while some of the skin panels are stiffened by stringers along the wing span. The wing has a rectangular planform with 6 m semi-span and 1.6 m chord length. Finite element model of the wing is prepared at Abaqus 6.7.1 and is composed of linear shell and beam elements. The model is shown in figure 4.1 [6], and consists of 17,070 linear quadrilateral elements of shell type, 1264 linear line elements of beam type, total element number of 18,334 and 16,024 nodes, thus 96,144 degrees of freedom. In all members of the structure, aluminium is employed with Young's modulus E=70000 MPa, Poisson ratio ν=0.33, density ρ=2700 kg/m^3, yield strength σ_{yield}=400 MPa. As a cantilevered boundary condition, all of the degrees of freedom at the root of the wing are set to zero. The aerodynamic load that will be applied to the wing is supplied from a computational fluid dynamics (CFD) analysis performed for the initial design. An Euler inviscid flow analysis by using Fluent commercial software was performed for Mach= 0.3 at sea level. For the sake of simplicity, the obtained total lift force of approximately 25,000 N is then expressed as an elliptic lift function which changes along the wing span but assumed to be constant along the chord [6].

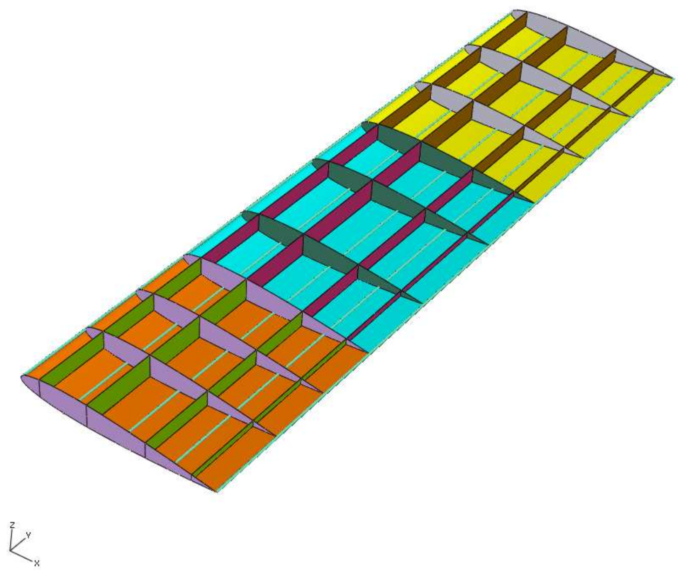

Figure 4.1: Computational model of the wing structure [6]

4.3.1 Deterministic Optimization of the Aircraft Wing

In this work, the physical design parameters are defined as independent functions of some abstract optimization variables for computational simplicity. The optimization variables will cover structural parameters such as cross sectional and thickness dimensions of the structural elements and some shape parameters.

The optimization criteria can cover the structural behavior descriptors such as mass, displacements, stresses, strains, and modal frequencies.

The deterministic optimization problem that will be solved has two objectives as minimization of weight and maximization of the first modal frequency of the structure while constraining maximum Von Mises stress with the yield strength of the material. A factor of safety is not used on the stress constraint in the deterministic optimization.

$$
\begin{aligned}
&\min_{\mathbf{s}\in\mathbf{S}} M(\mathbf{s}), \quad \max_{\mathbf{s}\in\mathbf{S}} f_1(\mathbf{s}) && && \textbf{(4.3)}\\
&g_1(\mathbf{s}) = \frac{\sigma_{yield}}{\sigma_{max}(\mathbf{s})} - 1 && \geq 0, \quad g_1(\mathbf{s}) \in \mathbf{R}\\
&g_2(\mathbf{s}) = \frac{u_0}{u_{max}(\mathbf{s})} - 1 && \geq 0, \quad g_2(\mathbf{s}) \in \mathbf{R}\\
&g_3(\mathbf{s}) = 1 - \frac{f_1^0}{f(\mathbf{s})} && \geq 0, \quad g_3(\mathbf{s}) \in \mathbf{R}\\
&g_4(\mathbf{s}) = \frac{M_0}{M(\mathbf{s})} - 1 && \geq 0, \quad g_4(\mathbf{s}) \in \mathbf{R}
\end{aligned}
$$

where M($\mathbf{s}$) is the total mass, $u_{max}(\mathbf{s})$ and $\sigma_{max}(\mathbf{s})$ are the maximum displacement and maximum Von Mises stress of the wing structure. $u_0 = 187$mm and $M_0 = 330$kg are chosen as reference values from the reference wing to constrain the displacement and mass. $f_1(\mathbf{s})$ is the first natural frequency of the structure, while $f_1^0 = 4.35$ Hz is the first natural frequency of the reference wing.

4.3.2 Definition of Optimization Variables

Since ribs, spars and skin panels are modeled as shell elements, the thicknesses of these elements and the diameter of the stringers are chosen as design parameters. The thicknesses of spars, ribs and skin panels are divided into three groups along the wing span, introducing 9 design variables. The outer diameter of all the stringers are kept constant along the span and expressed as only one design parameter while the wall thickness of the stringers are taken as one over third of the outer diameter. In figure 4.1, the structural components of the wing and the thickness parameters related to these components are presented so that each different color shows a different design parameter.

The computational time that will be spent for optimization will be shortened if the number of optimization variables that will be used in the optimization loop can be reduced by using abstract optimization variables. Therefore, four abstract optimization variables k_1,k_2,k_3,k_4 are used to describe 9 design variables related to the thicknesses of all spars, ribs and stringers. The relation between design parameters and abstract optimization variables are as follows;

$$t_{A1} = k_1 k_2 k_3 \tilde{t}_{A1} \qquad t_{A2} = k_2 k_3 k_4 \tilde{t}_{A2} \qquad t_{A3} = k_3 k_4 k_1 \tilde{t}_{A3} \tag{4.4}$$

where, t_{A1}, t_{A2}, t_{A3} are the physical design variables describing the skin panel thicknesses for the three partitions along the span. t_{A1} is chosen to be on the cantilevered side. $\tilde{t}_{A1}$, $\tilde{t}_{A2}$, $\tilde{t}_{A3}$ are the reference values for the thicknesses of the three type skin panels which are dictated in the initial wing design. Similarly;

$$t_{B1} = k_1 k_2 k_3 \tilde{t}_{B1} \qquad t_{B2} = k_2 k_3 k_4 \tilde{t}_{B2} \qquad t_{B3} = k_3 k_4 k_1 \tilde{t}_{B3} \tag{4.5}$$

where, t_{B1}, t_{B2}, t_{B3} are the physical design variables describing the spar thicknesses for the three partitions along the span. t_{B1} is chosen to be on the cantilevered side. $\tilde{t}_{B1}$, $\tilde{t}_{B2}$, $\tilde{t}_{B3}$ are the reference values for the thicknesses of the three spar partitions which are dictated in the initial wing design. Finally;

$$t_{C1} = k_1 k_2 k_3 \tilde{t}_{C1} \qquad t_{C2} = k_2 k_3 k_4 \tilde{t}_{C2} \qquad t_{C1} = k_3 k_4 k_1 \tilde{t}_{C3} \tag{4.6}$$

where, t_{C1}, t_{C2}, t_{C3} are the physical design variables describing the rib thicknesses for the three partitions along the span. t_{C1} is chosen for the first rib on the cantilevered side. $\tilde{t}_{C1}$, $\tilde{t}_{C2}$, $\tilde{t}_{C3}$ are the reference values for the thicknesses of the three different rib groups which are dictated in the initial wing design. In addition, two more design variables, the stringer outer diameter d_0 and the inner wall thickness of the stringer beam t_w are:

$$d_0 = k_4 \tilde{d}_0 \qquad t_w = \frac{d_0}{3} \tag{4.7}$$

where d_0 is the reference diameter value of the initial wing design. The abstract optimization variables are chosen to be less than one so that the inital rough structure will be forced to get lighter. The lower and upper limits of the abstract optimization variables are determined as:

$$0.8 \leq k_1 \leq 1.0 \tag{4.8}$$

$$0.6 \leq k_2 \leq 1.0 \tag{4.9}$$

$$0.4 \leq k_3 \leq 1.0 \tag{4.10}$$

$$0.2 \leq k_4 \leq 1.0 \tag{4.11}$$

In addition, the location of the first four ribs which is the group on the wing root side and also the location of the middle two spars are chosen to be variable. The absolute distance from the root to each of the first four ribs are chosen as four optimization variables y_1,y_2,y_3,y_4 . For two middle spars, the ratio of the distance between the leading edge of the wing to the spar divided by the chord length is chosen as two dimensionless optimization variables c_1,c_2. Thus, 16 independent design variables are introduced at all.

$$500\text{mm} \leq y_1 \leq 800\text{mm} \qquad 2150\text{mm} \leq y_4 \leq 2800\text{mm} \tag{4.12}$$

$$900\text{mm} \leq y_2 \leq 1300\text{mm} \qquad 0.25 \leq c_1 \leq 0.45 \tag{4.13}$$

$$1400\text{mm} \leq y_3 \leq 1950\text{mm} \qquad 0.55 \leq c_2 \leq 0.75 \tag{4.14}$$

A rather bulk wing initial design will be given for the optimization problem since abstract variables are chosen as such to reduce the thicknesses in any ways. At the initial configuration, $\tilde{t}_{A1} = \tilde{t}_{A2} = \tilde{t}_{A3} = 5$mm, $\tilde{t}_{B1} = \tilde{t}_{B2} = \tilde{t}_{B3} = 20$mm, $\tilde{t}_{C1} = \tilde{t}_{C2} = \tilde{t}_{C3} = 16$mm, $y_1 = 600$mm, $y_2 = 1100$mm,$y_3 = 1600$mm, $y_4 = 2250$mm, $c_1 = 0.35$, $c_2 = 0.65$.

4.3.3 Reliability Based Design Optimization of the Aircraft Wing

A structural optimization problem similar to the one in equations **(4.3)** will be solved with two random variables which are Young Modulus E and yield strength σ_{yield} of the material. Thus, the constraints concerning stress (g_1), displacement (g_2) and frequency (g_3) in those equations become probabilistic constraints due to their dependencies on the random variables vector $\mathbf{X} = [E \quad \sigma_{yield}]$

Young's Modulus E of the material and yield strength σ_{yield} are modeled with normal distributions using N(70000, 350) MPa and N(400, 20) MPa. Thus, the optimization problem can be formulated as;

$$
\begin{aligned}
&\min_{\mathbf{s}\in\mathbf{S}} M(\mathrm{s}), \quad \max_{\mathbf{s}\in\mathbf{S}} f_1(\mathbf{X},\mathbf{s}) && && && (4.15)\\
&g_1^{prob}(\mathbf{X},\mathbf{s}) = \frac{\sigma_{yield}(\mathbf{X})}{\sigma_{max}(\mathbf{X},\mathbf{s})} - 1 && \geq 0, && g_1^{prob}(\mathbf{X},\mathbf{s}) && \in \mathbf{R}\\
&g_2^{prob}(\mathbf{X},\mathbf{s}) = \frac{u_0}{u_{max}(\mathbf{X},\mathbf{s})} - 1 && \geq 0, && g_2^{prob}(\mathbf{X},\mathbf{s}) && \in \mathbf{R}\\
&g_3^{prob}(\mathbf{X},\mathbf{s}) = 1 - \frac{f_1^0}{f(\mathbf{X},\mathbf{s})} && \geq 0, && g_3^{prob}(\mathbf{X},\mathbf{s}) && \in \mathbf{R}\\
&g_4^{det}(\mathbf{s}) = \frac{M_0}{M(\mathbf{s})} - 1 && \geq 0, && g_4(\mathbf{X},\mathbf{s}) && \in \mathbf{R}
\end{aligned}
$$

4.3.4 Optimization Framework

During the optimization process Abaqus-6.7.1 is used to compute the structural response of the structural system and AMV method code written in MATLAB is used to evaluate the random variables. In order to perform an optimization study, a workflow should be prepared in Modefrontier to govern the optimization process. In this workflow the optimization variables (with their upper and lower bounds and incrementations), scheduler, design of experiments, objectives, constraints, output variables and the softwares are defined. Optimization workflow is prepared to automate the multiobjective multidisciplinary optimization problem. Once the workflow is run, it controls the optimization process automatically by using the well prepared script files and models. Figure 4.6 shows the workflow of this optimization problem. In this workflow, Modefrontier's script files drive Abaqus node in batch mode. In each optimization iteration, Modefrontier updates the thickness parameters of the wing and create a new input file for Abaqus and MATLAB. In MATLAB, Abaqus is called twice for each reliability analysis iteration to calculate the gradient of the stress constraint: Once for y_{plus} (design point plus step size h) and once for y_{minus} (design point minus step size h). In this way, by running Abaqus from the MATLAB code depending on the random variable E, maximum stress of the wing is calculated and the gradients of the stress constraint is computed in that loop by *central finite difference approximation*. The output of the MATLAB reliability code provides updated values of Young's Modulus and yield stress. Finally, this output file is used by Abaqus to calculate the desired values of displacement, frequency, mass and maximum stress for deterministic optimization. For reliability analysis, target reliability index is chosen as $\beta_t = 3$. A parallel type of system is considered when the stress and displacement constraints are treated. For the sake of simplicity, stress constraint is considered to be dominant for reliability analysis. Figure 4.2 is a simple representation of the implemented workflow.

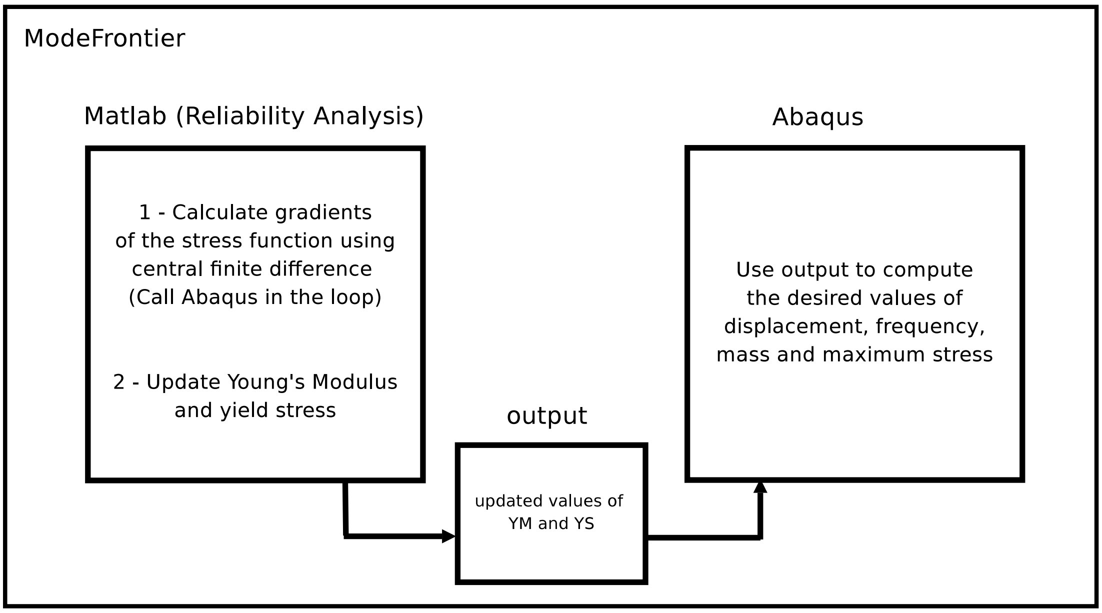

Figure 4.2: Workflow of the optimization problem

4.4 Results and Discussion

In the aircraft wing study, 24 design of experiments (DOE) with "Sobol sequence" are used and 300 maximum number of iterations per subiterations for the NLPQLP (an algorithm based on SQP) are defined. Sobol sequence distributes the experiments uniformly in the design space. Finally, a total number of 171 designs are generated for the optimization problem. Solution of the problem took about 85 hours on a workstation with Intel(R) Core(TM)2 Quad CPU

6700@2.40 GHz processor and 2GB of RAM on Microsoft Windows XP operating system. 65 designs were found to be feasible that satisfy the constraint condition. Furthermore, there are 10 error designs. As a result, 3 designs are found in the pareto front set for this optimization problem. These paretos are demonstrated in table 4.1 and in figure 4.3. The first design in table 4.1 is selected

Table 4.1: Paretos from RBDO

Pareto	Mass (kg)	Frequency (Hz)
1	291.47	5.7084
2	291.51	5.7087
3	291.61	5.7075

Table 4.2: Paretos from Deterministic Optimization

Pareto	Mass (kg)	Frequency (Hz)
1	282.23	5.2682
2	282.65	5.2691
3	282.77	5.2658

as the optimum design due to its cumulative improvement concerning both objectives. Table 4.4 demonstrates those improvements after reliability based design optimization with respect to the reference values of $M_0 = 330$kg and f_1^0 $=$ 4.35 Hz. Here, both objectives are evaluated with equal weight, i.e. %50 importance for each is taken into account. Other design engineers may choose among these three designs according to their needs. Moreover, the designs which

Table 4.3: Comparison of Deterministic and Probabilistic Optimization Results

	Deterministic Optimization	Probabilistic Optimization
Mass (kg)	282	291
Frequency (Hz)	5.26	5.70

are found previously in the deterministic optimization process in [6] are given in table 4.2. Briefly, table 4.3 shows the difference between deterministic and probabilistic optimization analysis. The results demonstrate that the mass of the reliability based designed wing has to be greater compared to the wing of the deterministic optimization in order to obtain a safer design. Furthermore, it

Table 4.4: Cumulative Improvements for Multicriteria Decision

Mass (kg)	Imp. in M. (%)	Frequency (Hz)	Imp. in F. (%)	Cumu. Imp. (%)
291.47	11.6750	5.7084	31.2275	21.4512
291.51	11.6636	5.7087	31.2344	21.4490
291.61	11.6333	5.7075	31.2068	21.4200

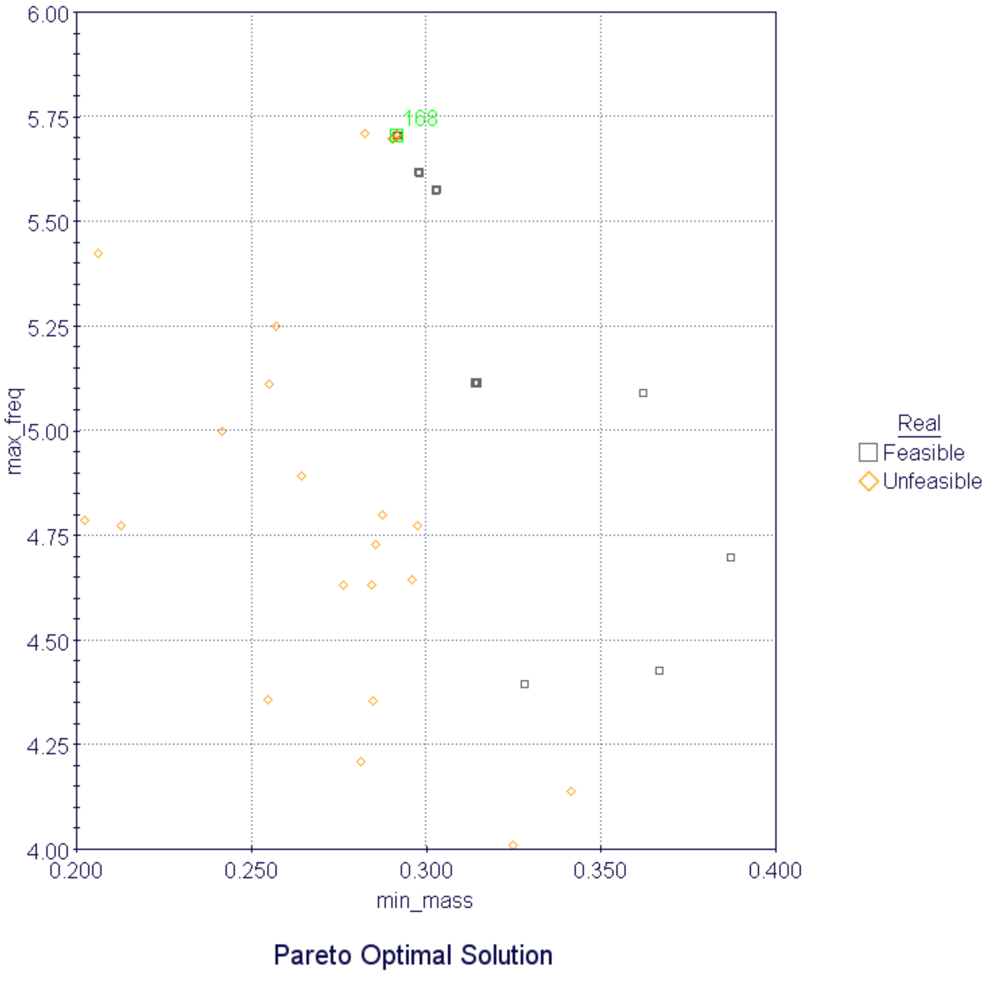

Figure 4.3

can be observed that the first natural frequency also increased after RBDO when compared to the deterministic optimization. As can be seen in the figures 4.4 and 4.5, thicknesses of the structural members decrease from the edge to the root

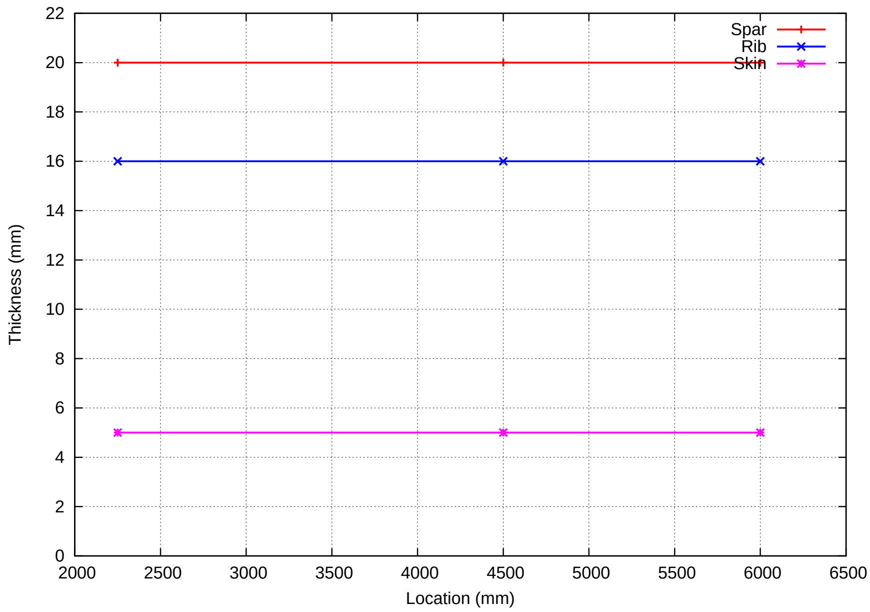

Figure 4.4: Locations and Thicknesses of Wing Structure Members Before Optimization

of the wing in order to increase the inertia of the wing structure. Therefore, depicted results explain the increase in frequency clearly and compromise with the expectations.

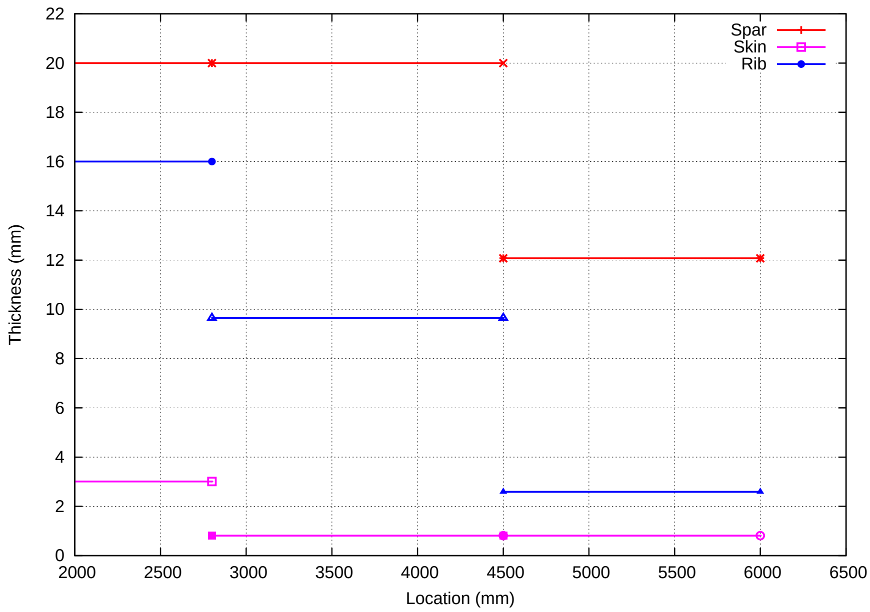

Figure 4.5: Locations and Thicknesses of Wing Structure Members After RBDO

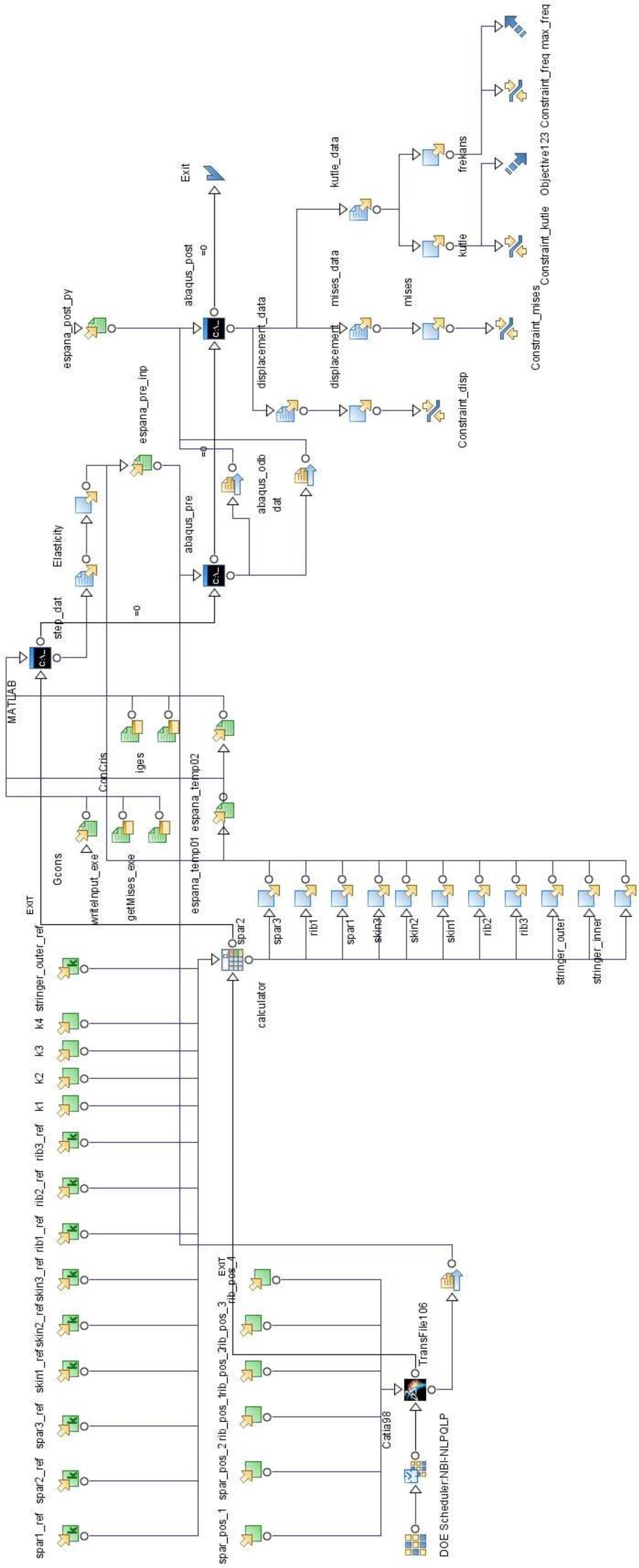

Figure 4.6: ModeFrontier Workflow

5. CONCLUSION

In this work, reliability-based design optimization is investigated and some of the related solution methodologies are explained, coded and implemented in MATLAB. Finally, MATLAB code and Abaqus are integrated in a ModeFrontier framework to solve an optimization problem concerning an aircraft wing. The results can be summarized as the following:

- Reliability analysis can be performed much more effectively using *Performance Measure Approach* compared to *Reliability Index Approach.* Due to its efficiency, PMA is preferred in solving the problems. Relevant methods to PMA are introduced and validated using some example problems from the literature before proceeding to the major problems.

- In chapter 3, both deterministic and probabilistic optimizations of a cantilever beam are performed. Here, stress and displacement constraints are calculated analytically. The results given in literature are obtained with perfect accuracy with MATLAB code. This beam problem is also solved in a ModeFrontier framework where the reliability analysis code written in MATLAB is coupled with Abaqus for stress computation. ModeFrontier produced very close optimization outputs using the integration of reliability analysis part of MATLAB code and Abaqus.

- At last, a multi-objective design optimization problem of an aircraft wing is reevaluated following the developed approach. RBDO results are proved to be acceptable when the results of first evaluation (i.e. deterministic optimization) of the same problem are considered.

- To the best of the author's knowledge, commercial finite element analysis tools such as Abaqus and Nastran do not include reliability analysis modules.

Therefore, the integration of the reliability analysis code written in MATLAB and Abaqus is the most remarkable novelty of this work.

- As the main inference, it is observed that RBDO method exhibits superiorities to deterministic optimization when dealing with uncertainties in the design process.

- Future work for this study may include using more complicated models and improving the capabilities of reliability analysis code: First, the system integration of multiple probabilistic constraints has to be implemented. Next, more effective methods such as second-order reliability method (SORM, based on MPP) or Latin Hypercube Sampling (LHS, one of the most efficient sampling methods) may be implemented and performed. Furthermore, reliability analysis algorithms based on a sequential single-loop can be preferred to overcome the potential computational burden. Parallel computing is another effective solution where applicable.

REFERENCES

[1] **Allen, M.**, 2004. *Reliability-Based Design Optimization of Multiphysics, Aerospace Systems*, Ph.D. thesis, University of Colorado, The Department of Aerospace Engineering Sciences.

[2] **Agarwal, H.**, 2004. *Reliability-Based Design Optimization: Formulations and Methodologies*, Ph.D. thesis, University of Notre Dame, The Department of Aerospace and Mechanical Engineering.

[3] **Nikolaidis, E.**, **Ghiocel, D. M. and Singhal, S.**, 2005. *Engineering Design Reliability Handbook*, CRC Press.

[4] **Youn, B. D.**, **Choi, K. K. and Park, Y. H.**, 2003. Hybrid Analysis Method for Reliability-Based Design Optimization, *Journal of Mechanical Design*, **125(2)**, 221–232.

[5] **Sues, R.**, **Aminpour, M. and Shin, Y.**, 2001. Reliability-Based Multidisciplinary Optimization for Aerospace Systems, *Proc. 42nd AIAA/ASME/ASCE/AHS/ASC Structures, Structural Dynamics, and Materials Conference, 16-19 April, Seattle, WA, USA*, AIAA.

[6] **Nikbay, M.**, **Yanangönül, A.**, **Öncü, L. and Koçaş, M.**, 2008. Multi-objective and gradient based structural design optimization of an aircraft wing, *Second International Conference on Multidisciplinary Design Optimization and Applications, 2 - 5 Sep 2008 , Gijon, Spain*, ASMDO.

[7] **Zou, T. and Mahadevan, S.**, 2006. A Direct Decoupling Approach for Efficient Reliability-Based Design Optimization, *Structural and Multidisciplinary Optimization*, **31 (3)**, 190–200.

[8] **Liu, H.**, **Chen, W. and Sheng, J.**, 2003. Application of the Sequential Optimization and Reliability Assessment Method to Structural Design Problems, *ASME Design Engineering Technical Conferences and Computers and Information in Engineering Conference, Anonymous American Society of Mechanical Engineers, Chicago, IL, United States, 2 A: 63–72*, ASME.

[9] **Hover, F. S. and Triantafyllou, M. S.**, 2006. Application of Polynomial Chaos in Stability and Control, *Automatica*, **42**, 789–795.

[10] **Smith, A. H. C.**, 2007. *Robust and Optimal Control Using Polynomial Chaos Theory*, Ph.D. thesis, University of South Carolina.

[11] **Mathellin, L.**, **Hussaini, M. Y. and Zang, T. A.**, 2005. Stochastic Approaches to Uncertainty Quantification in CFD Simulations, *Numerical Algorithms*, **38**, 209–236.

[12] **Knioa, O. M. and Maitre, O. P. L.**, 2006. Uncertainty Propagation in CFD Using Polynomial Chaos Decomposition, *Journal of Fluid Dynamics Research*, **38**, 616–640.

[13] **Choi, S. K.**, **Grandhi, R. V.**, **Canfield, R. A. and Pettit, C.L.**, 2004. Polynomial Chaos Expansion with Latin Hypercube Sampling for Estimating Response Variability, *AIAA*, **42 (6)**, 1191–1198.

[14] **Youn, B. D. and Choi, K. K.**, 2004. An Investigation of Nonlinearity of Reliability-Based Design Optimization Approaches, *Journal of Mechanical Design*, **126**, 403–411.

[15] **Li, H. and Foschi, R. O.**, 1998. An Inverse Reliability Method and its Application, *Structural Safety*, **20 (3)**, 257–270.

[16] **Youn, B. D.**, **Choi, K. K. and Du, L.**, 2004. Enriched Performance Measure Approach (PMA+) for Reliability-Based Design Optimization, *Proceedings 10th AIAA/ISSMO MAO Conference*, AIAA.

[17] **Yang, R. J. and Gu, L.**, 2004. Experience with Approximate Reliability-Based Optimization Methods, *Structural and Multidisciplinary Optimization*, **26**, 152–159.

[18] **Du, X. and Chen, W.**, 2004. Sequential Optimization and Reliability Assessment Method for Efficient Probabilistic Design, *Journal of Mechanical Design*, **126 (2)**, 225–233.

[19] **Thanedar, P. B. and Kodiyalam, S.**, 1991. Structural Optimization Using Probabilistic Constraints, *Proceedings of the 32nd AIAA/ASME/ASCE/AHS/ASC Structures, Structural Dynamics and Materials Conference, 8-10 April, New York, NY, USA*, AIAA.

[20] **Tu, J.**, **Choi, K. K. and Park, Y. H.**, 2001. Design Potential Method for Robust System Parameter Design, *AIAA Journal*, **39 (4)**, 667–677.

[21] **Chen, X.**, **Hasselman, T. K. and Neill, D. J.**, 1997. Reliability Based Structural Design Optimization for Practical Applications, *Anonymous AIAA*, **4**, 2724–2732.

[22] **Royset, J. O.**, **Kiureghian, A. D. and Polak, E.**, 2001. Reliability-Based Optimal Structural Design by the Decoupling

Approach, *Reliability Engineering and System Safety*, **73 (3)**, 213–221.

[23] **Tu, J.**, **Choi, K. K. and Park, Y. H.**, 1999. A New Study on Reliability-Based Design Optimization, *Journal of Mechanical Design*, **121**, 557–564.

[24] **Li, F. and Wu, T.**, 2008. *d-RBDO: A Deterministic Approach for Reliability Based Design Optimization*, Ph.D. thesis, Arizona State University, Department of Industrial Engineering.

[25] **Sues, R. H. and Cesare, M. A.**, 2000. An Innovative Framework for Reliability-Based MDO, *AIAA*.

[26] **Bowman, K.**, **Granddhi, R. and Eastep, F.**, 1989. Structural Optimization of Lifting Surfaces with Divergence and Control Reversal Constraints, *Structural Optimization*, **1**, 153–161.

[27] **Friedmann, P.**, 1991. Helicopter Vibration Reduction Using Structural Optimization with Aeroelastic/Multidisciplinary Constraints - A Survey, *Journal of Aircraft*, **28**, 8–21.

[28] **Barthelemy, J. F.**, **Wrenn, G.**, **Dovi, A. and Hall, L.**, 1994. Supersonic Transport Wing Minimum Design Integrating Aerodynamics and Structures, *Journal of Aircraft*, **31**, 330–338.

[29] **Dovi, A. R.**, **Wrenn, G. A.**, **Barthelemy, J. F. M.**, **Coen, P. G. and Hall, L. E.**, 1995. Multidisciplinary Design Integration Methodology for a Supersonic Transport Aircraft, *Journal of Aircraft*, **32 (2)**, 290–296.

[30] **Jha, R. and Chattopadhyay, A.**, 1999. Multidisciplinary Optimization of Composite Wings Using Refined Structural and Aeroelastic Analysis Methodologies, *Engineering Optimization*, **32**, 59–78.

[31] **Tzong, G.**, **Baker, M.**, **D-Vari, R. and Giesing, J.**, 1994. Aeroelastic Loads and Structural Optimization of a High Speed Civil Transport Model, *5th AIAA/NASA/USAF/ISSMO Symposium on Multidisciplinary Analysis and Optimization, Panama City Beach, FL, AIAA Paper No 94-4378*, AIAA.

[32] **Maute, K.**, **Nikbay, M. and Farhat, C.**, 2001. Coupled Analytical Sensitivity Analysis and Optimization of Three-Dimensional Nonlinear Aeroelastic Systems, *AIAA*, **39 (11)**, 2051–2061.

[33] **Rosenblatt, M.**, 1952. Remarks on a Multivariate Transformation, *Annals of Mathematical Statistics*, **23(3)**, 470–472.

[34] **Coleman, T. F. and Li, Y.**, 1996. An Interior, Trust Region Approach for Nonlinear Minimization Subject to Bounds, *SIAM Journal on Optimization*, **6**, 418–445.

[35] **Byrd, R. H.**, **Gilbert, J. C. and Nocedal, J.**, 2000. A Trust Region Method Based on Interior Point Techniques for Nonlinear Programming, *Mathematical Programming*, **89 (1)**, 149–185.

[36] **Arora, J. S.**, 2004. *Introduction to Optimum Design*, 2nd Edition, Elsevier Academic Press.

[37] *Abaqus 6.7 Version Documentation*, Simulia.

[38] *Modefrontier V4 Version Documentation*, Esteco.

[39] **Nikolaidis, E.**, **Ghiocel, D. M. and Singhal, S.**, 2008. *Engineering Design Reliability Applications: For the Aerospace, Automative and Ship Industries*, CRC Press.

[40] **Gnedenko, B. and Ushakov, I.**, 1995. *Probabilistic Reliability Engineering*, John Wiley and Sons, Inc.

[41] **Youn, B. D. and Choi, K. K.**, 2004. A New Response Surface Methodology for Reliability-Based Design Optimization, *Computers and Structures*, **82**, 241–256.

[42] **Robinson, D. G.**, 1998. *A Survey of Probabilistic Methods Used in Reliability, Risk and Uncertainty Analysis: Analytical Techniques I*, Sandia National Laboratories.

[43] **Frangopol, D. M. and Maute, K.**, 2003. Life-Cycle Reliability-Based Optimization of Civil and Aerospace Structures, *Computers and Structures*, **81**, 397–410.

[44] **Eggert, R. J.**, 1991. Quantifying Design Feasibility Using Probabilistic Feasibility Analysis, *17th Design Automation Conference presented at the 1991 ASME Design Technical Conferences, New York, NY, USA, 32: 235–240*, ASME.

[45] **Parkinson, A.**, **Sorensen, C. and Pourhassan, N.**, 1993. General Approach for Robust Optimal Design, *Journal of Mechanical Design*, **115**, 74–80.

[46] **Hohenbichler, M.**, **Gollwitzer, S. and Kruse, W.**, 1987. New Light on First- and Second Order Reliability Methods, *Structural Safety*, **4**, 267–284.

[47] **Koyluoglu, H. U. and Nielsen, S. R. K.**, 1994. New Approximations for SORM Integrals, *Structural Safety*, **13**, 235–246.

[48] **Hasofer, A. M. and Lind, N. C.**, 1974. Exact and Invariant Second-Moment Code Format, *Journal of the Engineering Mechanics*, **100**, 111–121.

[49] **Chen, W. J.**, **Allen, K. and Tsui, K.**, 1996. Procedure for Robust Design: Minimizing Variations Caused by Noise Factors and Control Factors, *Journal of Mechanical Design*, **118**, 478–485.

[50] **Sues, R. H.**, **Oakley, D. R. and Rhodes, G. S.**, 1995. Multidisciplinary Stochastic Optimization, *Anonymous ASCE*, **2**, 934–937.

[51] **Koch, P. N.**, **Simpson, T. W. and Allen, J. K.**, 1999. Statistical Approximations for Multidisciplinary Design Optimization: The Problem of Size, *Journal of Aircraft*, **36**, 275–286.

[52] **Paez, T. L. and Hunter, N. F.**, 2000. *Nonlinear System Modeling Based on Experimental Data*, Sandia National Laboratories.

[53] **Choi, K.**, **Lee, G.**, **Yoon, S. J.**, **Lee, T. H.**, **Choi, D. H.**, **Choi, B. L. and Choi, J. H.**, 2008. A Sampling-based Reliability-Based Design Optimization Using Kriging Metamodel with Constraint Boundary Sampling, *12th AIAA/ISSMO Multidisciplinary Analysis and Optimization Conference, 10 - 12 September 2008, Victoria, British Columbia Canada*, AIAA.

[54] **Manan, A. and Cooper, J. E.**, 2008. Uncertainty of Composite Wing Aeroelastic Behaviour, *12th AIAA/ISSMO Multidisciplinary Analysis and Optimization Conference, 10 - 12 September 2008, Victoria, British Columbia Canada*, AIAA.

CURRICULUM VITAE

Name Surname: Çağrı Ulucenk

Place and Date of Birth: İzmir, 1983

Permanent Adress: Şükrü Saracoğlu Cad., 277 Sok.,
No: 10, K: 2, D: 2, 35280, Üçyol, İzmir

Universities and
Colleges Attended: Ege University, Mathematics

Publications:

- Nikbay M., Ulucenk Ç., Yanangönül A. and Aysan A., 2009: Reliability-Based Multi-Objective Design Optimization of an Aircraft Wing Structure with Abstract Optimization Variables. 5^{th} *Ankara International Aerospace Conference*, August 17-19, 2009, METU, Ankara, Turkey.